

Acoustic Transmission Techniques in the Development of Porosity and Osteoporosis Measurement Systems

Lawrence Yule

MSc Applied Acoustics
Southampton Solent University

ABSTRACT

A review of the current methods for testing for osteoporosis has been carried out, followed by porosity, to evaluate their strengths and weaknesses, and show how a new low-cost testing method could benefit the early onset detection of osteoporosis. The method has then been derived from a review of stress wave testing methods, which are primarily used to detect damage to trees or structures, measuring differences in the speed of sound transmission through impulse or impact, as well as the resonant frequency of the sample (among other properties). Measurement methods are described that can be used to detect a change in the speed of sound transmission caused by changes to porosity within a wooden dowel sample. A shaker and force transducer were first used to generate and measure a force applied transversally (perpendicular to the surface) to a solid sample, the transmitted wave was then captured by measuring acceleration on the surface of sample a set distance away from the impulse. Results showed that when the porosity was increased by drilling, the speed of sound was reduced. Attachment via a screw meant that this method would be destructive to the sample, and so the shaker was replaced by an impact hammer. A National Instruments LabView system has been used to acquire the signals using a USB oscilloscope, reliably calculate the speed of sound transmission, and save the data to file. Results for measurements taken with the impact hammer showed that an increase in porosity causes a reduction to the speed of sound transmission, with an average change of $-19.12 \pm 5.68 \text{ m/s}$ per 1% increase in the porosity of a pine wood sample, and a t-stat p-value of <0.05 , showing a high statistically significant difference between the means. Regression analysis shows that the change is very close to linear, with an average r^2 value of $r^2=0.98931$ across the 3 distances measured. The system could be improved in the future with more powerful acquisition hardware, and a more repeatable testing procedure, which could potentially be adapted for use on humans to detect variations in bone density caused by osteoporosis.

Table of Contents

1. INTRODUCTION	4
2. LITERATURE REVIEW	5
2.1. Osteoporosis	5 - 6
2.2. Dual X-ray Absorptiometry	6
2.3. Quantitative Computed Tomography	7
2.4. Ultrasound	8
2.5. Porosity	9
2.6. Stress Wave Testing	9 - 10
3. RESEARCH METHOD	11
3.1. Preliminary Test Method	11
3.1.1. Equipment	12 - 13
3.1.2. Test Method	13
3.1.2.1. Sample Selection & Transducer Attachment	14
3.1.2.2. Signal Generation	14
3.1.2.3. Data Acquisition	15
3.2. Measurement Method For Impact Excitation	16
3.2.1. Equipment	16
3.2.2. Test Method	17
3.2.3. Calculation of Porosity	18
3.2.4. Sample Selection & Transducer Attachment	18
3.2.5. Data Acquisition	19
3.2.5.1. National Instruments LabView	19 - 21
4. RESULTS	22
4.1. Preliminary Results	22 - 24
4.2. Impact Hammer Measurement Results	25
4.2.1. Speed of Sound Tables	25 - 26
4.2.2. Box Plots	26 - 27
4.2.3. Regression Plots	28 - 29
5. DISCUSSION	30 - 32
6. CONCLUSION	33
7. REFERENCES	34 - 37
8. APPENDICIES	38 - 50

1 INTRODUCTION

This study aims to investigate how the transmission of sound or vibration through a material can be analysed and used to measure variations in porosity, potentially leading to the development of a low cost early detection system for osteoporosis that could be installed in a doctor's surgery or medical centre.

Osteoporosis is a condition that weakens bones, making them brittle and easier to break or fracture from even minor falls. This condition has no external symptoms making it imperative that it is detected as early as possible, in an attempt to prevent it from worsening. Current systems used in the detection and measurement of osteoporosis have been evaluated, identifying the methods used in the determination of parameters such as bone density, and the speed of sound transmission. The relative costs and availability of these methods have been considered, leading to the proposed low cost system that could be used in early detection. Previous studies involving the transmission of sound or vibration through a material have also been investigated in order to identify the most applicable transducer type, placement, and signal parameters.

In order to measure the variations in porosity of a material a testing system has been devised that utilises acoustic signals transmitted through or along the structure of a material between measurement transducers. The transmitted signals can be analysed and, in the case of osteoporosis, the results for a particular patient can be compared to the results of a healthy person for use in determining if the patient has osteoporosis, and if they should be referred for further evaluation. A number of experiments using different transducer and signal combinations have been carried out on wooden dowels of varying porosity to determine if the test procedures are capable of detecting a change in porosity, and which combination allows for the smallest variation in porosity to be detected. The results of these experiments have subsequently been analysed and conclusions have been drawn as to the viability of this method for the measurement of porosity and osteoporosis.

The hypothesis for this study is as follows:

Null (H0): The test method is not able to reliably measure a change to the speed of transversal sound transmission through a wooden dowel when the porosity of the sample has been increased.

Alternative (H1): The test method is able to reliably measure a change to the speed of transversal sound transmission through a wooden dowel when the porosity of the sample has been increased.

The null hypothesis can be rejected if there is a consistent and measurable difference between signals that have passed through pieces of wood with varying porosities.

In the next section the literature relating to the areas of research in question have been evaluated and reviewed, leading to the development of a research methodology. This is followed by the experimental results of each test method, and an analysis of each of them. Suggestions have been made on further research that could potentially contribute to producing a low cost early detection system.

2 LITERATURE REVIEW

In this section, a literature review has been carried out in order to identify the most relevant research that relates to this study into low frequency osteoporosis measurement.

A background to osteoporosis has been provided which covers: what the condition is, who is affected by it, the causes of it, and the effects it has on the body. This is followed by an overview of the currently used diagnosis systems, investigating their measurement methods and the parameters used in the determination of osteoporosis. For each of the systems their strengths and weaknesses have been evaluated to determine where it may be possible to make improvements to be used in the development of a new measurement system.

The next section focuses on porosity, which is linked to how osteoporosis affects bone. The methods used for measuring porosity have been identified, with emphasis placed on investigating the techniques used and specifically methods which are non-destructive to the test sample. This information will guide the development of test system which can be used to measure osteoporosis through the measurement of porosity, which will need to be non-destructive when eventually used on humans.

The final section of this literature review investigates methods of transmitting and analyzing low frequency signals passed through a sample to determine its quality, or a number of other structural properties. There is a limited amount of research regarding the low frequency transmission of waves through bone, although some have been identified. The review mostly focuses on methods of “stress wave testing” which is a non-destructive (in most cases) method of determining the structural properties of wood. This method of analysis may be possible to modify for use in investigating the structural properties of bone, which may be affected by osteoporosis.

2.1 Osteoporosis

Osteoporosis is a skeletal condition affecting both the density and the structural integrity of bone. The condition causes an increased fracture risk, most commonly found in the hip, vertebrae, and wrist. There is a steep increase in fracture risk with age, which is more commonly found in women than men (Cooper and Christodoulou, 2003). Women are more likely to experience osteoporosis due to having around 30% less peak bone mass than men, as well as having an increase in bone loss after the menopause (Christiansen, 1995). The lifetime risk of hip fracture as a result of osteoporosis in the United States and northern Europe is between 11% and 18%, and sufferers of the condition are likely to receive fractures caused by osteoporosis in other areas of the body over their life time (Kanis *et al.*, 2009). The condition has also been shown to affect the white population more than non-whites, making it a major issue in the UK population which was last recorded in the 2011 national census as being 86% white (*Ethnicity and national identity in England and wales 2011*, 2015). Around 300,000 people in the UK suffer from fractures each year, which is predicted to double by 2050 (British Orthopedic Association, 2007). The financial and health related costs of osteoporosis are expected to rise as the global population ages, with current estimates predicting that by 2020 osteoporosis will cost the UK over £2.1 billion per year (Burge *et al.*, 2001).

The condition is defined by the World Health Organisation based on bone mineral density (BMD) T-scores taken at the hip, which has been shown to be a strong predictor of osteoporotic fracture. In post-menopausal women a diagnosis is met if their BMD T-score is ≤ -2.5 . For men the same threshold is used for ages above 65. For younger men/women, other risk factors must be present before a diagnosis of osteoporosis is given. Although BMD is a strong indicator of osteoporosis it is still only a guide, as many fractures occur outside of this T-score range (Singer, 2006).

Bone mass can be measured in a number of different locations, such as the forearm, hip, spine, and heel using multiple methods. Unfortunately this is complicated by the fact that each area has a different bone structure, as well as having different loss rates of bone mass. Despite this it has been shown that there is notable correlation between the measurement of osteoporosis at one site and another (Christiansen, 1995).

2.1.1 Dual X-ray Absorptiometry

Dual X-ray Absorptiometry is the most common method of measuring BMD, and is mostly used on central locations of the body, such as the spine and hip. It measures the density of bone in g/cm^2 which can be compared to the mean result for healthy young adults to determine whether it fits the WHO diagnosis criteria (which is based on DXA measurements). Because the calculation of BMD uses an area and not a volume it cannot be considered a true representation of density, and so is sometimes referred to as areal bone mineral density (Singer, 2006).

The system works by measuring the attenuation of two different X-ray energies simultaneously, one for measuring the attenuation of bone mineral (hydroxyapatite) and one for measuring the attenuation of soft tissue. Bone mineral results can be used in the diagnosis of osteoporosis, while soft tissue results can be used in other body composition studies. The boundaries of the scanned bone are found using an edge detection algorithm, at which point all of the Bone Mineral Content (BMC) measurement results between these boundaries are mean averaged and divided by the area of bone being measured, producing a value of areal Bone Mineral Density (BMD) in g/cm^2 (Blake and Fogelman, 1997).

For healthy subjects the precision of measurements is very good, with a SD of around $0.01\text{g}/\text{cm}^2$, although this worsens with obesity, and as bone density decreases. When used in osteoporosis diagnosis the difference between a particular result and a reference result of young healthy bone, or other results for the same age range, in terms of T/Z score, is preferred to a calculation of absolute value. Reference data is provided by the manufacturers of DXA devices, which vary significantly, meaning that a diagnosis can vary depending on the device used (Laskey, 1996).

Scan times and radiation dose vary depending on the type of x-ray beam used. A DXA machine that uses a pencil beam will take longer to scan an area of interest but will give a smaller dose of radiation than using a wide angle fan beam. This makes fan beam systems unsuitable for use on children (Fewtrell, 2003). Unfortunately the diagnosis thresholds based on T-scores given by the WHO only apply to the older population and not for young adults or children, meaning that DXA results cannot be used to indicate a fracture risk in younger people as there is not a relevant threshold for comparison. Younger people are often being referred for DXA scans which may lead to an incorrect diagnosis and the possibility of subsequent unnecessary treatment (Fewtrell, 2003). The equipment required for DXA measurement is expensive and the procedure requires a radiographer, which means it cannot be found in all medical centers or hospitals (Singer, 2006).

2.1.2 Quantitative Computed Tomography

Quantitative Computed Tomography is a method of measuring bone mineral density (BMD). It differs from DXA in that the results are given volumetrically (g/cm^3) rather than arealy (g/cm^2), and that other properties of bone can also be analysed in 3 dimensions (Blake and Fogelman, 1997).

The system uses CT scanners, which produce an image based on the absorption of x-rays that pass through the body. Areas of the body with a comparatively high density, such as bone, will absorb more x-rays than the surrounding tissue. All scanners are calibrated to the X-ray absorption of water, which is set to 0, and measured in Hounsfield Units (HU). In order to convert from HU to bone density (g/cm^3) a bone mineral phantom is included when scanning, this contains a number of materials (notably hydroxyapatite) that absorbs x-rays a similar amount to that of bone, which the patient's result can be compared to. Spatial resolution is high enough in most cases that cortical bone can be distinguished from trabecular bone, meaning that a bone density can be measured for each of them independently, or the cortical bone can be ignored (Adams, 2009).

Either full body CT scanners or more specialised scanners for use in specific areas of the body may be used which have been specifically developed for bone density measurements. When using a full body scanner measurements are generally taken at the spine or hip, while peripheral scanners can take measurements on the forearm or tibia. CT Measurements give more structural information about bone than DXA, which can give more information than just BMD in regards to skeletal strength and the risk of fracture. (Engelke *et al.*, 2007).

QCT induces a higher radiation dose than DXA when used on the spine or hip, although it is still considered a small dose when compared to other X-ray imaging methods. When peripheral CT scanners are used, on the wrist for example, the radiation dose is considered negligible, which allows for their use on children.

As CT scanners are used for medical imaging not related to the diagnosis of osteoporosis they are in high demand, meaning that patients may have difficulty in gaining access to them. There are a limited number of software packages available for extracting the density information from full CT images, which may also limit their availability in hospitals. Similar to DXA, QCT measurements require a trained radiographer to perform the scans and to analyse the results. (Singer, 2006).

The WHO diagnosis criteria used in DXA measurements of bone density cannot be applied to the measurements taken with QCT. The composite measurements of cortical and trabecular bone taken with a DXA scanner are not comparable with the single measurement of trabecular bone that is normally taken with a QCT scanner, as the QCT BMD score is likely to reduce more rapidly with age, which may lead to an over-classification of people with the condition if based on the WHO T-score criteria for DXA (Adams, 2009). DXA is the more commonly used measurement method based on its lower cost to hospitals and medical centers, its large research background, its lower radiation dose, and its approval by the WHO (Blake and Fogelman, 1997).

2.1.3 Ultrasound

Another method developed for examining the health of bone involves the use of ultrasound. This method is primarily used on the heel (calcaneus) as it is made of around 90% trabecular bone, the type of bone that is more sensitive to osteoporotic changes than the cortical bone that surrounds it. Measurements taken at the heel have been shown to correlate well to a risk of fracture at other sites, such as at the hip. The area is also easily accessible to transducers, making it a repeatable measurement system (Langton, 2011).

The test method consists of a transmitter and receiver placed either side of the heel, while either having the heel immersed in water, or with the transducers mounted via a gel. An ultrasonic signal is transmitted through the bone, and analysed for the amount of broadband ultrasound attenuation (BUA), as well as the speed of signal transmission (SOS). These two parameters can then be combined to give an estimate of the bone mineral density (BMD) at the heel (Frost, Blake, and Fogelman, 2001).

Measurement variability is mostly caused by the positioning of transducers, as the edges of bone can cause unwanted diffraction that affects the result. Another problem is the use of a comparison phantom, which are hard to produce with the correct attenuation values, and without them degrading due to immersion in water. Other factors such as changes in temperature can also affect the amount of ultrasound attenuation. The many commercially available systems all have different transducer setups and designs, leading to them all providing wildly different results. This makes their results hard to compare between and makes it difficult to distinguish which of the systems is the most effective. (Langton, 2011).

It has been shown that there is a large degree of error associated with the calculation of BMD using ultrasound techniques when compared to measurements taken using DXA, but the measurement of SOS and BUA can be used to gather other information relating to the structure of bone, and the related fracture risks (Faulkner *et al.*, 1994).

Ultrasound methods do not use any ionizing radiation, they are cheaper, and the equipment required to use them takes up less room than DXA or QCT methods. The systems also have an advantage in that they do not need a highly specialised person, such as a radiographer, to use and analyse the results (Prins *et al.*, 1997).

2.1.4 Porosity

In carrying out the measurement of porosity within porous materials there are currently a number of different test methods, most commonly the Archimedes' method that is specified in standards ISO2738 (ISO, 1999) and EN623-2 (British Standards Institute, 1993). The method described in these standards involves the immersion of the material under test in a fluid (oil for metals, deionised water for ceramics), which is a potentially destructive method to the sample, and cannot be carried out on a material in situ. Inaccuracies and issues with reproducibility can be found with this method due to the variations in results caused by differences in fluid densities between measurements (Yim-Bun *et al*, 2002). Other methods used for the measurement of porosity are more complex, involve immersion in other fluids, statistical analysis, or are only applicable to a limited number of materials (Unosson *et al*, 2014).

As already shown with the use of ultrasound methods, variations in porosity down to and smaller than 0.8% can be detected by measuring and analysing a transmitted signal (Michaels, *et al*. 1993). A low frequency method for measuring the porosity of porous materials is described by Dupont (2013) in which a sample of a material is placed within a transmission tube for testing, however this method is not purely experimental, but requires the knowledge of theoretical parameters at higher frequencies in order to determine the porosity.

2.1.5 Stress Wave Testing

In order to derive a test method that fits the low cost criteria of this study and provides results that are simple to analyse in comparison to the currently used osteoporosis detection methods, a review of the literature regarding low frequency acoustic signal transmission through materials has been carried out. This will identify the measurement parameters and techniques that it may be possible to utilize with the equipment available.

“Stress wave testing” has been identified as a term used to describe the process of measuring the transmission of a sound wave that has travelled through the structure of a material. The transmitted signal is then analysed to determine a number of parameters, in most cases the speed of sound transmission is used, as well as the resonant/natural frequency. This type of measurement system is generally used to identify damage to wooden objects, sometimes trees, and sometimes structures such as telephone poles or bridges. The systems generally use an impact or impulse, which is of a low frequency and could be analysed with inexpensive equipment, while also potentially being non-destructive to the sample under test.

Many non-destructive testing systems are commercially available, for use in the evaluation of standing trees for example (Chuang and Wang, 2001) or are currently used and described in research papers. The large majority of these focus on longitudinal transmission, whereby the sample is excited via an impact to one end, creating a compression wave. The transmitted signal is then measured using an accelerometer (in most cases) either placed at the other end of the sample, or placed on a side perpendicular to the impact. The wave transmission speed can then be used to calculate the Modulus of Elasticity (MOE) if the mass density of the sample is known. (Ross, 2015). The calculation of MOE has been shown to produce very similar results whether calculated from static bending techniques or stress wave testing (correlation coefficient $r=0.98$. Bell *et al*. (1954)).

The use of one-dimensional measurements using stress wave testing techniques has been proven to be effective for examining wave behavior in wooden beams by Bertholf (1965), Ross (1985) and Kaiserlik and Pellerin (1977). Pellerin *et al* (1985) and Rutherford (1987) carried out tests on wooden samples damaged by fungi, and discovered a strong correlation between the transmitted wave speed and compressive strength of the samples. It has been shown that the wave speed in wood is affected by a number of factors, notably the moisture content which increases the speed of sound transmission as moisture increases, and the quality of the wood, which reduces the speed of sound the more the wood is degraded. (Moavenzadeh, F. 1990).

There are a number of different types of stress wave testing. A pulsed echo system places the receiving transducer on the opposite side of a sample to the impact or impulse, measuring the time difference between reflected wave peaks to determine the speed of sound transmission. A pitch and catch system utilises 2 receiving transducer placed a set distance apart, from which the time difference between both waves can be used to calculate the wave speed. The transmitted waveforms will be heavily dependent on how the sample is supported, as well as how the transducers are mounted. (Ross, 2015).

In 1974, Hanagud tested bone samples using acoustic emission techniques to discover whether a change to the density of bone (through the removal of calcium) has an effect on transmitted signal. Results showed that a change was measureable but improvements to the system were needed in order to quantify the differences. Stress wave techniques have subsequently been used *in vivo* to measure the effect of osteoporosis on bone structure. Impulses created with an impact hammer and measured using an accelerometer after transmission through the tibia have been analysed to determine the natural frequency, showing a reduction with osteoporosis. These results correlated well with measurements taken using ultrasound methods (M. S. Holi, 2003). A similar system was used by Cheng (1995) to evaluate the effect of osteoporosis and age on the speed of sound transmission *in vivo*. Results showed that measuring variations in wave speed would be reliable enough detect changes to the mechanical properties of bone.

The outcome of this literature review has led to the development of a testing method for use in measuring variations in the porosity of wooden samples, based on non-destructive stress wave transmission methods, which could potentially be adapted for use in a low cost system for measuring changes to bone density caused by osteoporosis.

3 RESEARCH METHOD

The objectives of this research methodology are to investigate whether the transmission of sound/vibration can be used to detect variations in porosity of a material, and if so, how accurate the system is at measuring a change to sound transmission. This can then be linked to how osteoporosis affects the structure of bone, and it may be possible to adapt the methodology for use on humans.

Prior research that has been identified in the literature review indicates that there is limited number of non-destructive test methods used for the measurement of porosity. For that reason, this methodology will focus on a non-destructive method, which will also be advantageous when adapting the method for use on humans.

A number of non-destructive signal transmission methods have been used on standing trees using stress wave methods which it may be possible to adapt for use in this scenario. The transmitted signal can be analysed and compared to other transmissions in order to identify the variations between them.

In order to analyse a transmitted signal, first a signal must be applied to the object under test in a non-destructive manner, and subsequently measured after transmission through a portion of the object. The reviewed literature has identified a number of different methods, most notably using an impact hammer or force transducer for measuring the input to an object, and using an accelerometer to measure the output signal after a period of transmission through the structure of a material.

Preliminary measurements have been carried out to determine whether a variation in porosity is detectable by analyzing a transmitted signal. In this measurement a rigid connection via a screw has been made between an electromagnetic shaker, force transducer, and a wooden dowel (the test sample), sine wave bursts have then been transmitted through the dowel and measured with an accelerometer to determine whether changes made to the porosity of the dowel through drilling it will affect the transmitted signal.

Subsequent measurements have focused on the use of an impact as the excitation force by using an impact hammer, as this is non-destructive to the sample (unlike the rigid connection) and may be possible to adapt for use on humans in the detection of osteoporosis. As in the preliminary measurements the results have been analysed to see whether a change in porosity is detectable, and how small of a variation can be detected. The results of these measurements have been statistically analysed to identify whether they are reliable and give consistent results.

3.1 Preliminary Measurement Method

An experimental method is described below for the measurement of low frequency (<1000Hz) signal transmission through a wooden dowel. The speed of signal transmission and the amount of signal attenuation between two transducers has been measured and compared between transmission in a solid wooden dowel and transmission through a dowel with increased porosity.

3.1.1 Equipment

Table 1 - Equipment List for Preliminary Measurements

<i>Equipment Type</i>	<i>Name</i>	<i>Specification</i>
Permanent Magnet Shaker	LDS V201 (+ Fixed gain amplifier)	<u>Freq. Range:</u> 5Hz-12kHz
Force Transducer	PCB 208C01	IEPE <u>Freq. Range:</u> 0.01Hz-36kHz <u>Sensitivity:</u> 112,410mV/kN
Signal Conditioners	DJB Instruments VB/01 IEPE	4mA constant current supply at 18VDC
Accelerometer	MMF KS901.100	IEPE <u>Sensitivity:</u> 100mV/g
Oscilloscope	Picoscope 2204A USB (2 Channel)	<u>Bandwidth:</u> 10MHz <u>Vertical Resolution:</u> 8 Bits <u>Input Ranges:</u> $\pm 50\text{mV}$ - $\pm 20\text{V}$
Signal Generator	NTi Minirator MR-PRO	Signal generation File playback

The test system consists of a LDS V201 Permanent Magnet Shaker powered by a fixed gain amplifier. This is being fed signal via RCA cable from an NTi Minirator MR-PRO, which is being used to play back pre-generated sine pulses. The shaker has a PCB 208C01 force transducer mounted to it via a screw, which is in turn mounted to the measurement sample via a screw. The force transducer is connected to a DJB Instruments VB/01 signal conditioner (via BNC) that provides the IEPE conditioning it requires, and is subsequently connected to channel A of a Picoscope 2204A USB oscilloscope. An accelerometer, an MMF KS901.100, is also connected to its own signal IEPE signal conditioner and channel B of the oscilloscope. The oscilloscope connects to a pc via USB cable, and is operated via Picoscope software.

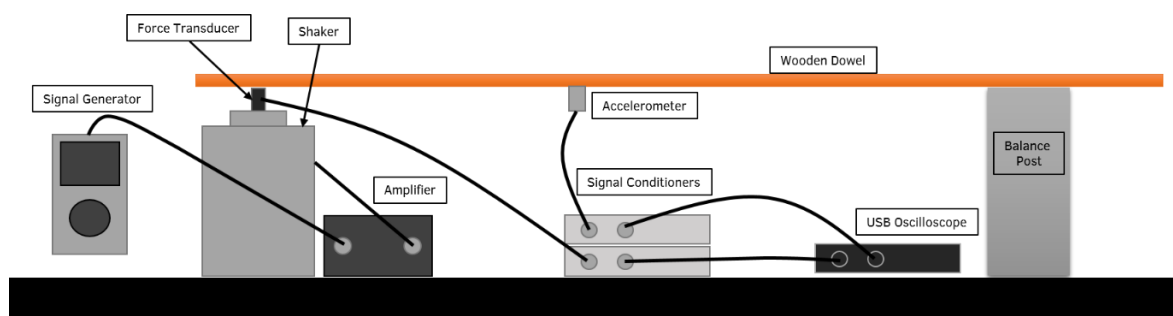


Figure 1 – Preliminary Measurement Setup Line Diagram

3.1.2 Test Method

The method has been derived from measurements carried out by Aygun *et al* (2014) on bone replicas using ultrasound transmission methods with the sample immersed in fluid, and from Fella *et al* (2003) who carried out porosity measurements on a sample in air using ultrasound. In both of these methods the transmitted signal has been analysed for variations caused by a number of different factors. It has been shown that variations in porosity and other properties of the material can have an effect on the amount of signal attenuation, and the speed of signal transmission, which can be used to derive other properties. This is also shown by Bekhta (2014) who analysed transmitted ultrasound signals using a non-destructive method to find the mechanical properties of composite woods. Compared to the methods used in the measurement of ultrasound propagation in bone replicas by Aygun *et al* (2014), this method does not require the sample to be immersed in a liquid (as also found in the Archimedes method for the measurement of porosity) as it will be carried out at lower frequencies, capable of being applied to the sample via impact or rigid connection.

In order to measure a signals input level when being applied to an object a force transducer or impact hammer may be used. In this case a force transducer has been preferred to an impact hammer in order to make the test more easily repeatable, as the force transducer can be mounted to a shaker providing repeatable signal output, unlike the use of an impact hammer which will have a variable impact level depending on how it is swung. A rigid connection with a screw also allows the distance between transducers to be kept constant, unlike using an impact hammer. An accelerometer is being used to measure the signal level after it has passed through the structure of the wood. This cannot be rigidly mounted to the surface of the dowel as it has a flat base, so double sided sticky tape has been used.

Measurements have been completed once on a solid dowel, then that same dowel has been drilled all the way along its length to increase its porosity. The dowel has then been re-tested. By using the same piece of wood for both tests any structural differences (such as varying densities, or the position/number of knots) that could affect the results have been eliminated.

3.1.2.1 Sample Selection & Transducer Attachment

An untreated wooden dowel was chosen as the test sample as it was cheap and easy to acquire, while also being easy to mount transducers to, and easily modifiable to increase porosity. A rectangular wooden dowel was chosen over a circular one to allow for a more repeatable attachment of transducers. The rectangular wooden dowel chosen has the dimensions: 15mmx15mmx750mm. This allowed enough surface area and thickness for the mounting of transducers, as well as enough length to carry out measurements at a number of different positions.

The dowel was rigidly attached to a force transducer (and shaker) via a screw (4mmD), which penetrated the surface of the wood by 7.5mm. The mounting was located 220mm from one end of the dowel, allowing accelerometer measurement positions of up to 500mm away. The accelerometer was attached to the centre of the flat side of the dowel with double sided sticky tape. Measurements were carried out along the surface of the wood, with the accelerometer placed on the same side as the attaching screw from the force transducer and shaker configuration.

3.1.2.2 Signal Generation

Test signals were generated in the software program Audacity on a Microsoft Windows PC, producing single cycle sine pulses at 40, 50, 63, 80, and 100Hz. The signals were exported as 16bit Wav files at maximum amplitude (0dBFS), and transferred to an NTi Minirator MR-PRO for playback through the shaker (via a fixed gain amplifier). The signals were then played back at a percentage of maximum output from the NTi Minirator. The levels were chosen based on which gave a suitable signal level without clipping, for all distances tested. These levels are shown below in Table 2:

Table 2 - Percentage output level per frequency

<i>Frequency (Hz)</i>	<i>Output Level (%)</i>
40	35.48
50	31.62
63	28.18
80	28.18
100	22.39

Measurements were carried out at distances 200, 300, 400, and 500mm away from the force transducer connection. Each measurement was taken 3 times to in order to carry out a mean average during data analysis.

The measurements were completed once on a solid dowel, then repeated on the same dowel after perforations had been made with a drill. Perforations were made with a 2.5mmD drill bit, at set positions along the dowel perpendicular to the surface, penetrating all of the way through on all sides. The perforation ratio was increased from 0% to 8.18%.

3.1.2.3 Data Acquisition

The signals from both the force transducer (input) and accelerometer (output) were simultaneously read into Picoscope software (v6) via a PicoScope 2204A 2 channel USB oscilloscope, capturing both signals after the level from the force transducer exceeded a trigger threshold. This data was then exported from the Picoscope software as a text file.

Table 3 - Oscilloscope Software Settings

<i>Parameter</i>	<i>Setting</i>
Input Range	±500mV (both channels)
Coupling Control	AC
Timebase	20ms/div
Sampling Rate	50MS/s (each channel)
Trigger Type	Rising Edge
Trigger Level	106.4mV
Pre-trigger	21%

The data from these measurements has been processed in Matlab, which was used to create plots showing the changes to the transmitted signal after the addition of perforations. Each plot shows a mean average of 3 measurements repeated immediately one after the other. The code used in the calculation of averages and the plotting of the graphs can be found in Appendix 1.

3.2 Measurement Method for Impact Excitation

A measurement method is described below for measuring the speed of sound transmission and frequency response of a transmitted signal through a material. The excitation force is applied via an impact hammer, and the transmitted signal is measured with an accelerometer. The measurement procedure is non-destructive to the sample.

The method has been derived from preliminary measurements and literature reviewed in the previous section. Using the preliminary method the excitation force was applied to the sample in a destructive manner, using a screw, which it would not be applicable to do in many cases. This method proved that an impulsive type signal (a single cycle of a sine wave) could be transmitted through a sample and would be measurable by an accelerometer. This is backed up by literature regarding stress wave testing methods currently employed to measure the structural properties of materials (Ross, 2015).

Using this method more data will be gathered in comparison to the previous measurements. The resolution and accuracy of the system has been evaluated to determine the variation in porosity that can be detected using speed of sound measurements.

3.2.1 Equipment

Table 4 - Impact Measurement Equipment

<i>Equipment Type</i>	<i>Name</i>	<i>Specification</i>
Accelerometer	MMF KS901.100	IEPE <u>Sensitivity:</u> 100mV/g
Impact Hammer	PCB 086C03	IEPE <u>Sensitivity:</u> 2.25mV/N
Data Acquisition	Picoscope 2204A	<u>Bandwidth:</u> 10MHz <u>Vertical Resolution:</u> 8 Bits <u>Input Ranges:</u> ±50mV-±20V
Software	National Instruments Labview 2014	

The test system consists of a an PCB 086C03 impact hammer connected to a DJB Instruments VB/01 signal conditioner (via BNC) that provides the IEPE conditioning it requires, and is subsequently connected to channel A of a Picoscope 2204A USB oscilloscope. An accelerometer, an MMF KS901.100, is also connected to its own DJB Instruments VB/01 IEPE signal conditioner and channel B of the oscilloscope. The oscilloscope connects to a pc via USB cable, and is operated via National Instruments LabView software.

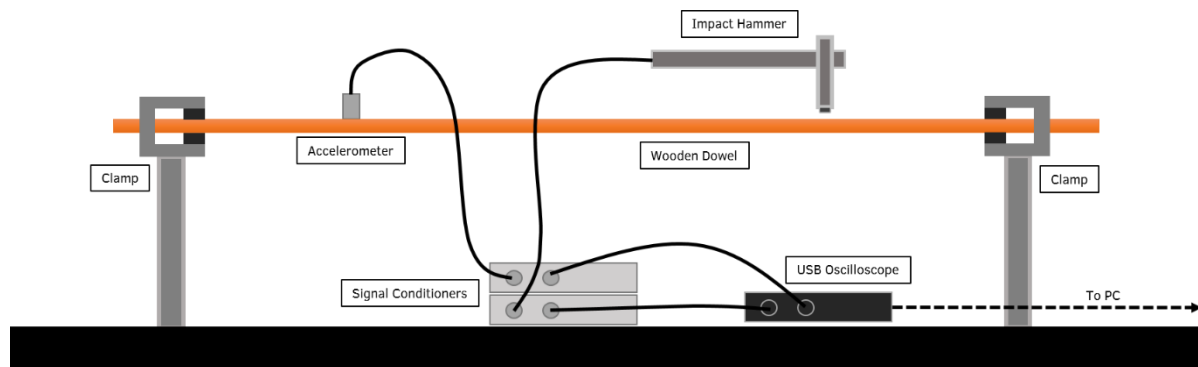


Figure 2 - Impact Measurement Line Diagram

3.2.2 Test Method

In this test the sample is a 1000mm x 15mm x 15mm piece of untreated pine, with no knots or noticeable damage. The sample has been fixed to a table at both ends with clamps in order to limit the resonances of the wood and keep the system damped as much as possible. The previous test showed that the response of the wood to stimuli was heavily dependent on the way it was mounted, with a greater number and higher amplitude of reflections occurring with less damping.

The test is to be carried out transversely, with an impulse from the impact hammer applied to the top surface of the wood, and the transmitted signal measured with an accelerometer placed at multiple distances along the same surface. Due to the impact force of the hammer being a large variable in this test, the force has been recorded to investigate what affect this has on the speed of sound transmission. This method of propagation was chosen as it most closely replicates the type of measurement that could be carried out on any specimen, especially those where the longitudinal transmission would be impossible to measure (e.g. through bone, standing trees, etc.).

The sample has been tested at multiple transmission lengths, 20, 30 and 40cm. For each distance, 25 measurements have been taken in order to identify a mean average, and standard deviation, giving an indication as to the accuracy of the method. The measurements have been repeated after increasing the porosity of the sample in 1% increments, up to a total of 5%.

3.2.2.1 Calculation of Porosity

Calculations of porosity can be found below:

Volume of test sample:

$$\text{Volume} = \text{Length} \times \text{Width} \times \text{Height}$$

$$\text{Volume} = 1000\text{mm} \times 15\text{mm} \times 15\text{mm}$$

$$\text{Volume} = 225000\text{mm}^3$$

Using a 2.5mmD drill bit, the amount of volume removed by a single hole:

$$\text{Volume of cylinder} = \pi \times r^2 \times h$$

$$\text{Volume of cylinder} = \pi \times 1.25\text{mm}^2 \times 15\text{mm}$$

$$\text{Volume of cylinder} = 73.63\text{mm}^3$$

The table below shows the amount of volume associated with 1,2,3,4, and 5% of the total volume, and how many holes need to be drilled to achieve it. The number of holes to be drilled has been rounded to the nearest whole number, to avoid having to drill multiple holes of different sizes.

Table 5 - Drill Hole Volumes & Porosity

Increase in porosity (%)	Volume (mm ³)	Number of holes drilled
1	2250	31
2	4500	61
3	6750	92
4	9000	122
5	11250	153

The holes have been evenly distributed over the whole sample, located centrally up to 3% porosity, and then spread across the width of sample for 4% and 5%. All drilled perpendicular to the surface.

3.2.2.2 Sample Selection & Transducer Attachment

As in the preliminary measurements a rectangular wooden dowel was chosen as it is easier to mount an accelerometer to a flat surface as opposed to a rounded one. The size of sample was kept the same (15mm x 15mm) but extended in length to 1000mm. The attachment method has been changed to “super glue”, as this provides a more repeatable connection than double sided tape, while still being non-destructive to the sample (in most cases). The accelerometer was placed in the centre of the dowel at each measurement position, and re-attached in the same location after each increase in porosity.

3.2.3 Data Acquisition

As in the previous measurement, a USB controlled oscilloscope has been used to measure the transmitted signals, but this time a National Instruments LabView system has been built to interface with the oscilloscope. Using a manufacturer provided SDK the system is able to capture the signals, detect the time difference between them, and record the speed of sound transmission automatically. The system can also be used to analyse the received signal in the frequency domain.

3.2.3.1 National Instruments LabView

Using the previous measurement methodology the speed of sound could not be determined from the results, only that there was a visible phase shift seen on the plotted signals after an increase in porosity. In order to measure the speed of sound, National Instruments LabView was chosen as it is capable of interfacing with the oscilloscope, acquiring the signals, calculating the results, and saving the captured data to file.

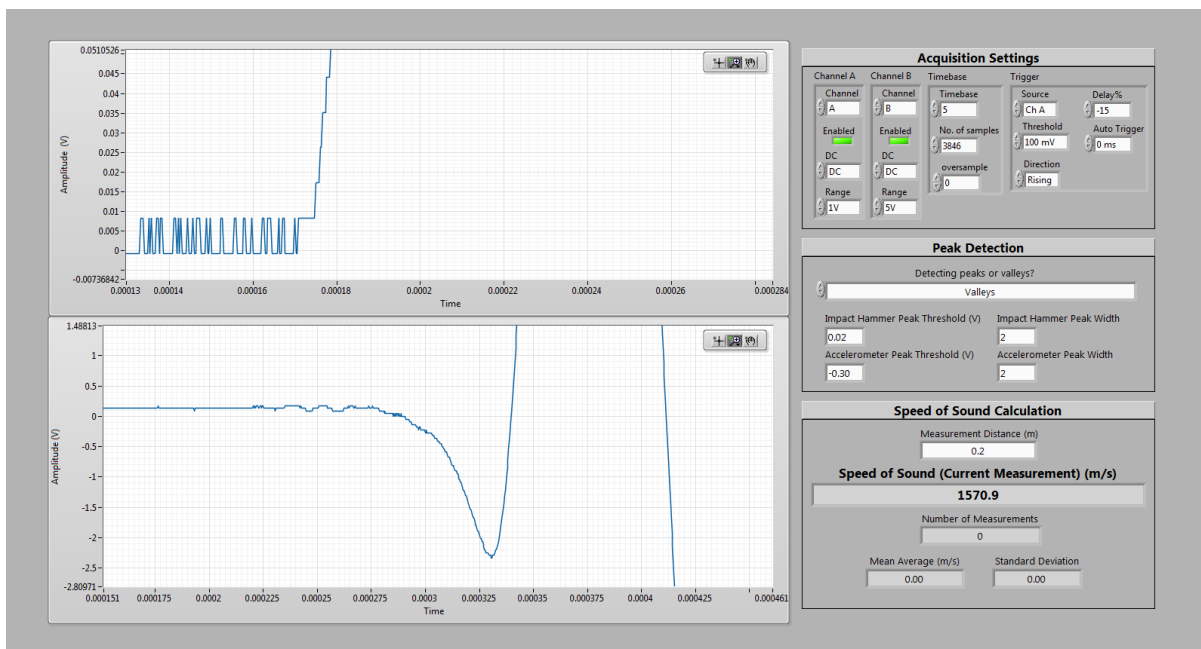


Figure 3 - National Instruments LabView Front Panel

The signals are acquired in much the same way as when using the Picoscope software from the previous measurement, the same parameters such as input range, sample rate and triggering can be selected, but LabView allows for the signals to be analysed after data capture. In this case a peak detection function has been used to identify the location in time that both signals deviate from 0, from which the time difference between them can be used in conjunction with the distance between transducers to calculate the speed of sound transmission. This data is then automatically saved to file, allowing for multiple measurements to be taken in quick succession. An option to save the waveform data is also included, so that it can be analysed in the frequency domain using fft.

The signals were first acquired using the Picoscope LabView SDK, which provided VI's that could read data from both input channels, set a trigger, select the appropriate timebase and sampling rate, and capture a block of data as waveforms. The settings for these parameters can be seen below in Table 6.

Table 6 - National Instruments LabView Acquisition Settings

Parameter	Setting
Channel A	DC, ±1V
Channel B	DC, ±10V
Timebase	8
No. Samples to Capture	3846
Oversample	0
Trigger Parameter	Setting
Threshold	100mV
Delay	-10%
Type	Rising

After capture the data was displayed on two waveform graphs (see Figure 3), where the onset of the input signal from the impact hammer and the onset of the signal from the accelerometer is shown. A peak detection VI was then used to detect the point at which the signals on both channels crossed a threshold, which was set to be slightly above 0V. The width of peak to be registered was set to 2 samples, as there was negligible noise on the signal that could interfere with the detection. The peak detection function has to be manually set to detect either peaks or valleys, for which a control can be seen on the front panel in figure 3.

After peak detection, the location in time of the first peaks to cross the set threshold was calculated by taking the first results from each of the peak arrays, and combining this with the associated time information taken from the waveforms. The time difference between the peaks was calculated by subtracting one from the other, giving the time between impact and arrival. This time difference was then used in the formula:

$$Speed (m/s) = \frac{Distance (m)}{Time (s)}$$

To calculate the speed of sound transmission. This is then stored in an array, whereby the next measurement taken is appended to it. This allows for a mean average and standard deviation to be calculated within LabView for however many measurements are taken. The input voltage of the impact hammer for each measurement is also saved to the array by using a Min & Max VI. The stored array is automatically saved to a text file for subsequent analysis.

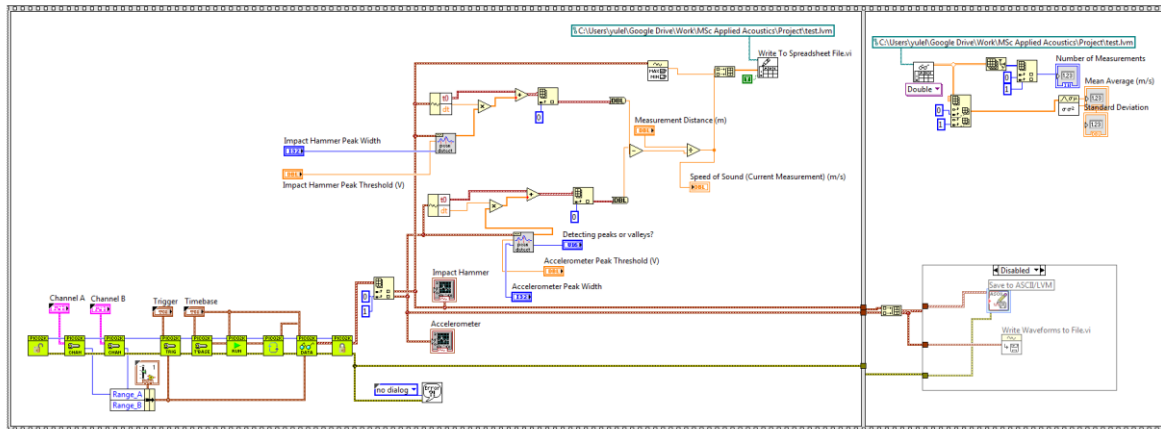


Figure 4 - National Instruments LabView Block Diagram

Due to the flexibility of the LabView test environment, the hardware used for data acquisition could be improved in the future to have (for example) a greater bit depth and higher sampling rate to allow for greater accuracy of measurement, without having to greatly modify the code. The disabled structure shown on the right of Figure 4 can be used to save the waveform data to file, for use in frequency analysis via fft or for data collection.

4 RESULTS

The results for preliminary measurements carried out using a shaker and force transducer on a wooden dowel can be found below (4.1) followed by the results of the measurements taken using an impact hammer (4.2).

4.1 Preliminary Measurement Results – Shaker/Force Transducer

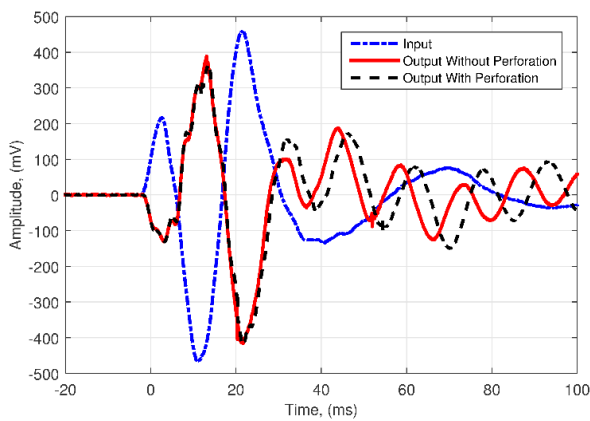
Results are plotted with a single input signal for both the perforated and non-perforated dowel measurements, as the input signal is the same for both tests and has been proven to be consistent after removing and reseating the dowel onto the attachment screw.

The signal received by the accelerometer is shown for both perforated and non-perforated measurements on each plot for comparison.

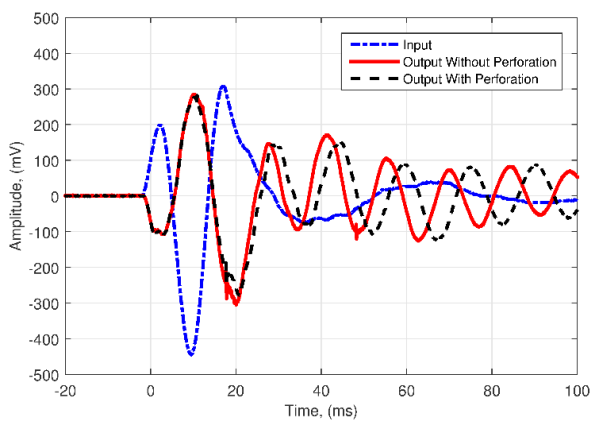
Results are shown for 200, 300, 400 and 500mm between transducers, at frequencies 40, 50, 63, 80 and 100Hz.

4.1.1 Measurements at 200mm

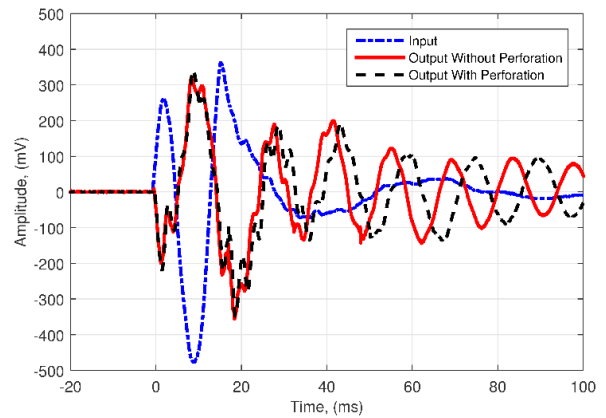
4.1.1.1 40Hz



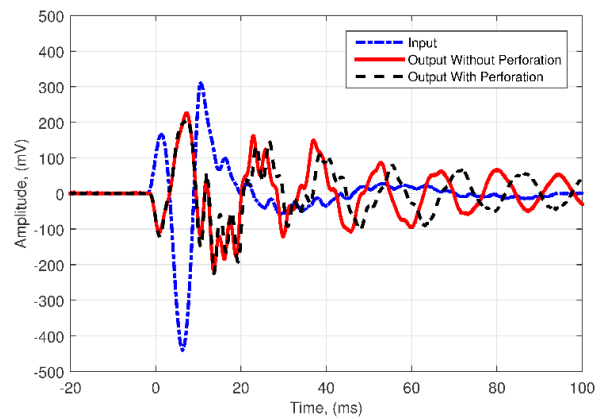
4.1.1.2 50Hz



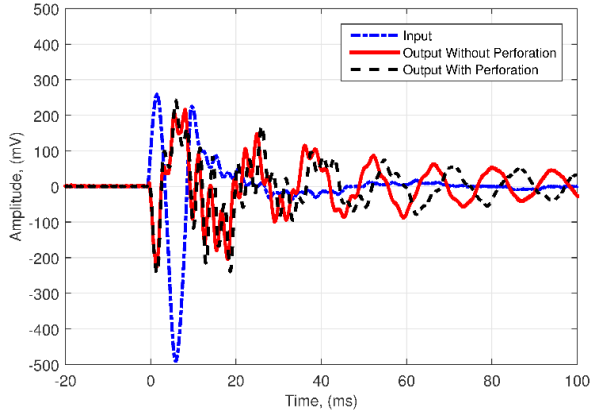
4.1.1.3 63Hz



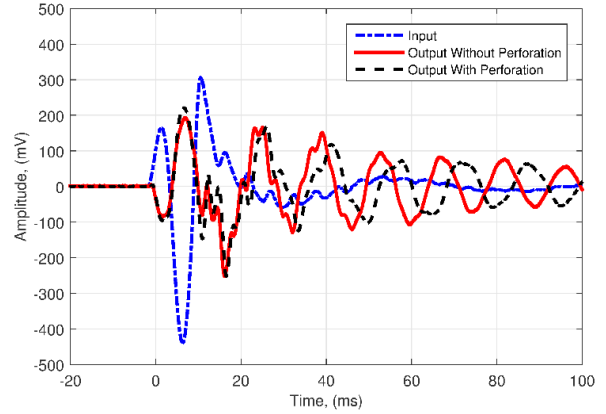
4.1.1.4 80Hz



4.1.1.5 100Hz

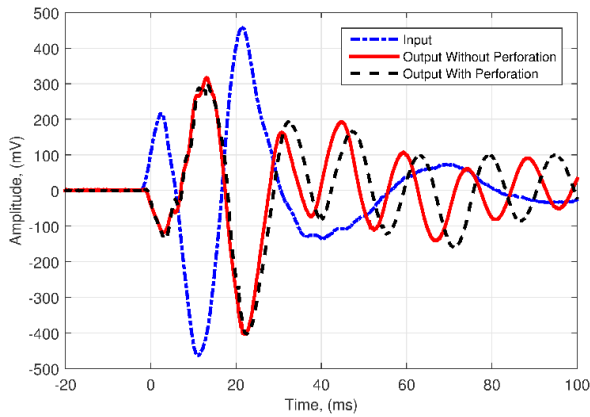


4.1.2.4 80Hz

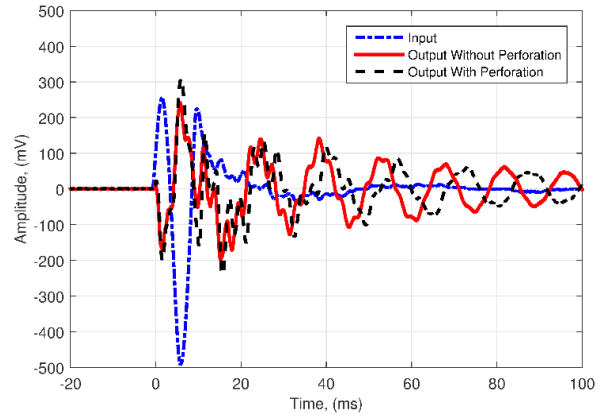


4.1.2 Measurements at 300mm

4.1.2.1 40Hz

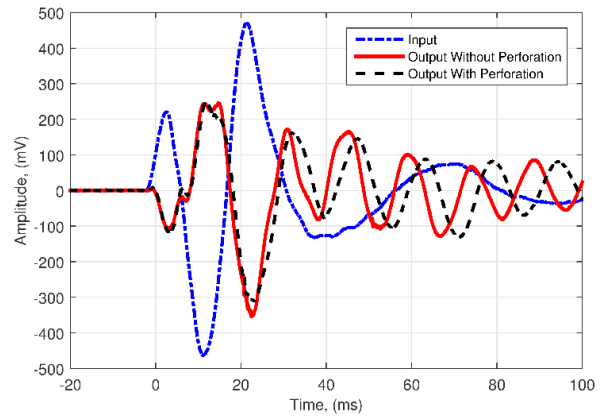


4.1.2.5 100Hz

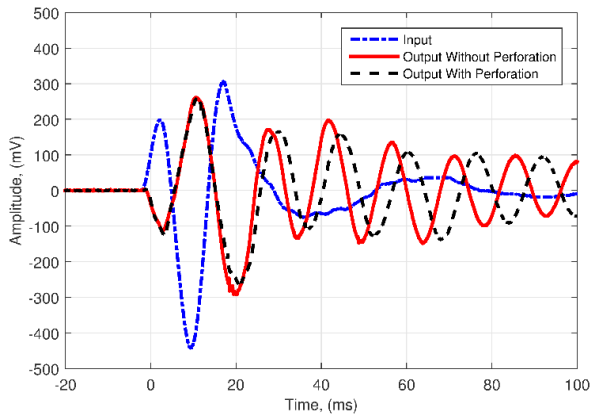


4.1.3 Measurements at 400mm

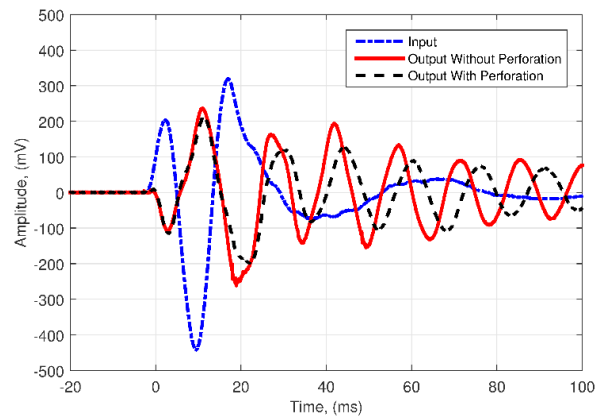
4.1.3.1 40Hz



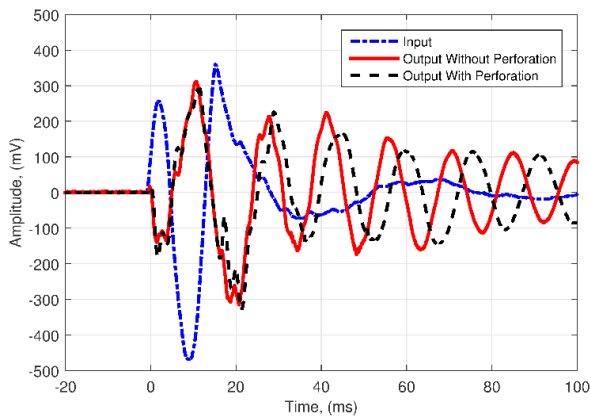
4.1.2.2 50Hz



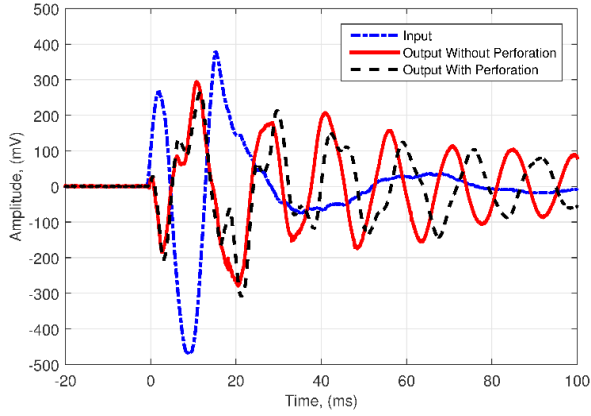
4.1.3.2 50Hz



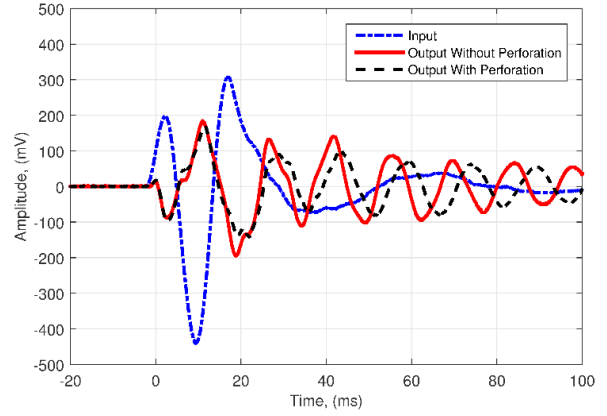
4.1.2.3 63Hz



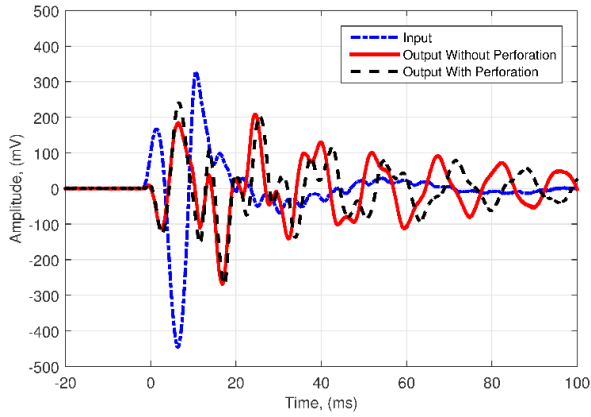
4.1.3.3 63Hz



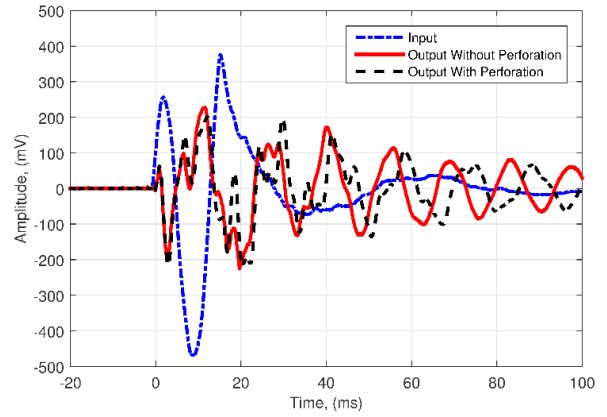
4.1.4.6 50Hz



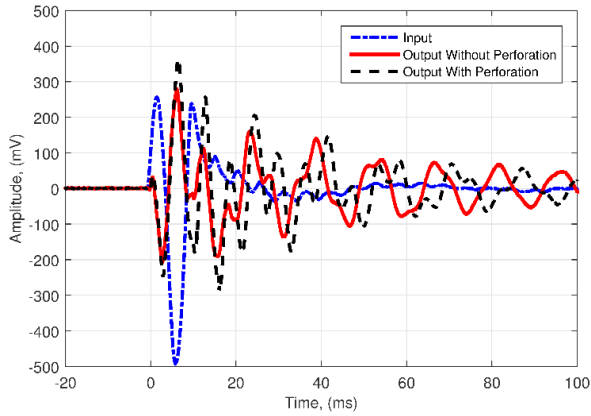
4.1.3.4 80Hz



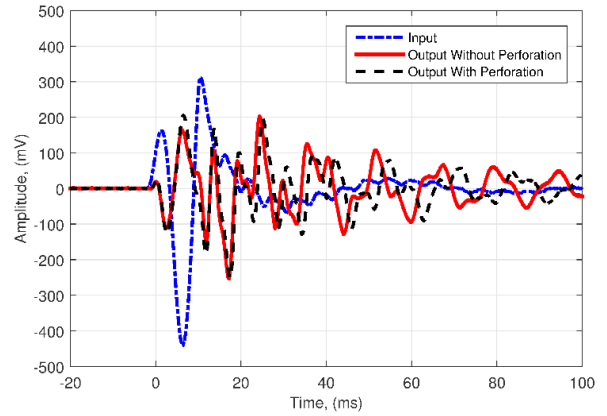
4.1.4.7 63Hz



4.1.3.5 100Hz

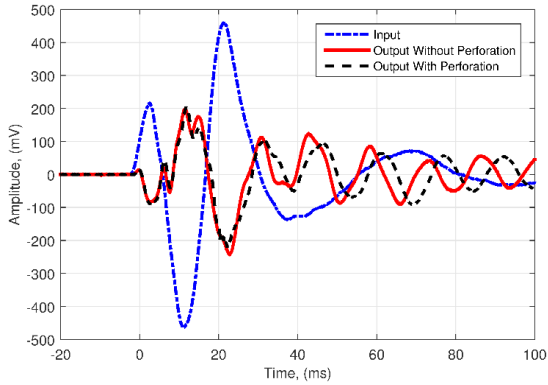


4.1.4.8 80Hz

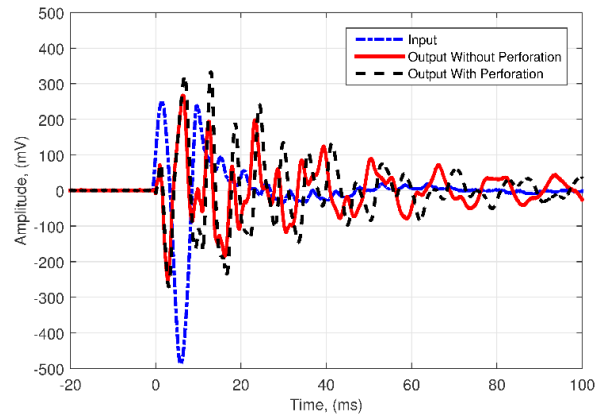


4.1.4 Measurements at 500mm

4.1.4.1 40Hz



4.1.4.9 100Hz



4.2 Impact Hammer Measurement Results

Results are shown for measurements of speed of sound transmission, along with the respective input force associated with each measurement. A mean average is shown for the 25 measurements taken at each of the 3 distances tested, along with the standard deviation. The change in the speed of sound transmission has also been calculated from the mean result for each porosity increment. The raw data used to produce these plots can be found in Appendix 8.2, along with f-tests and t-tests showing the statistical significance of the difference between means.

4.2.1 Speed of Sound Tables

The tables below show the measured speed of sound and standard deviation for each porosity, as well as the change to the speed of sound for each increment. The final column shows the average speed of sound change and standard deviation.

4.2.1.1 200mm

Porosity	Mean Speed of Sound (m/s)	Change in Speed (m/s)	Average Change (m/s)
0%	1696.95 ±19.69		
1%	1665.88 ±26.70	-31.07	
2%	1639.51 ±23.84	-26.37	
3%	1622.52 ±12.12	-16.99	-23.01 ±5.93
4%	1607.15 ±14.93	-15.37	
5%	1581.89 ±11.69	-25.27	

4.2.1.2 300mm

Porosity	Mean Speed of Sound (m/s)	Change in Speed (m/s)	Average Change (m/s)
0%	1636.81 ±13.59		
1%	1621.60 ±11.91	-15.21128	
2%	1605.50 ±18.14	-16.10072	
3%	1592.05 ±11.6	-13.44336	-16.19 ±2.01
4%	1575.48 ±19.96	-16.5758	
5%	1555.86 ±13.21	-19.61376	

4.2.1.3 400mm

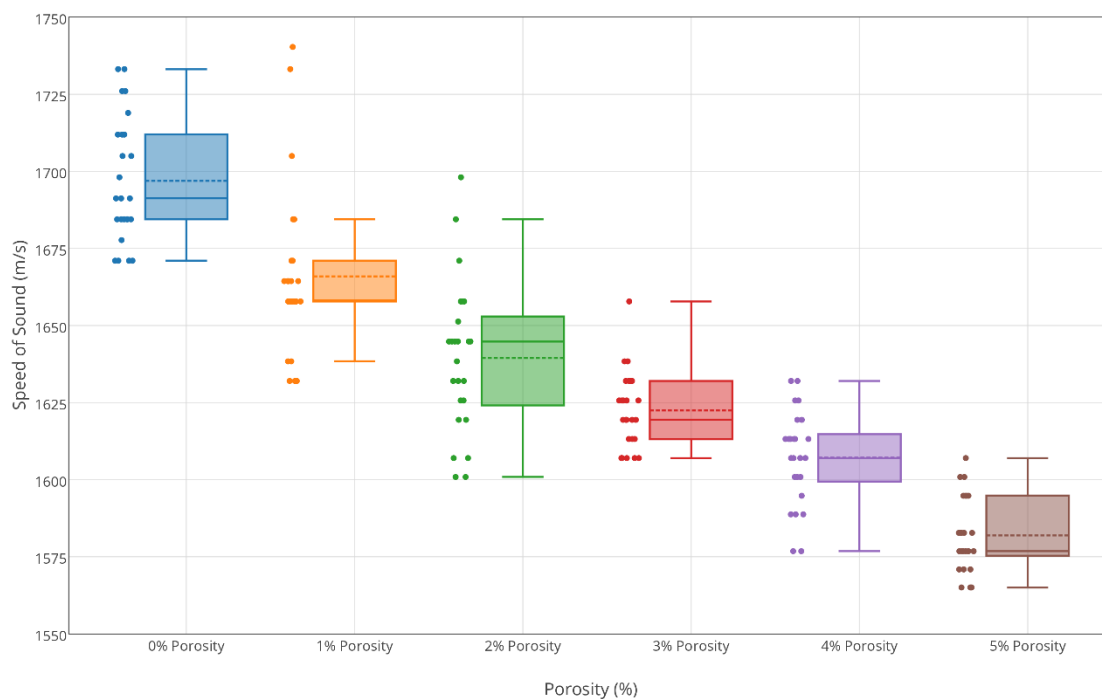
Porosity	Mean Speed of Sound (m/s)	Change in Speed (m/s)	Average Change (m/s)
0%	1577.26 ±26.81		
1%	1558.49 ±17.57	-18.77	
2%	1533.04 ±7.71	-25.45	
3%	1521.08 ±16.78	-11.96	-18.15 ±5.74
4%	1509.78 ±9.21	-11.31	
5%	1486.50 ±12.30	-23.28	

4.2.2 Box Plots

Box plots show the range of data points, interquartile range, median (solid line) and mean (dotted line), with the difference between the two showing the data skew. Data points outside of the range of the whiskers are considered outliers.

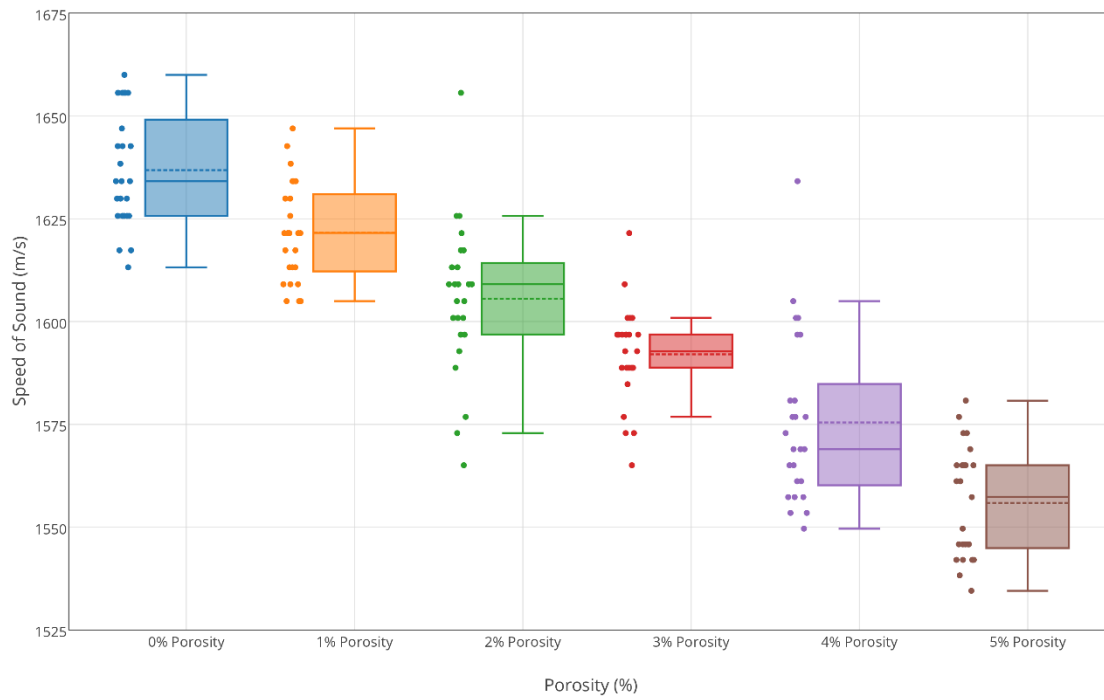
4.2.2.1 200mm

Speed of Transversal Sound Transmission Through 200mm of Pine Wood



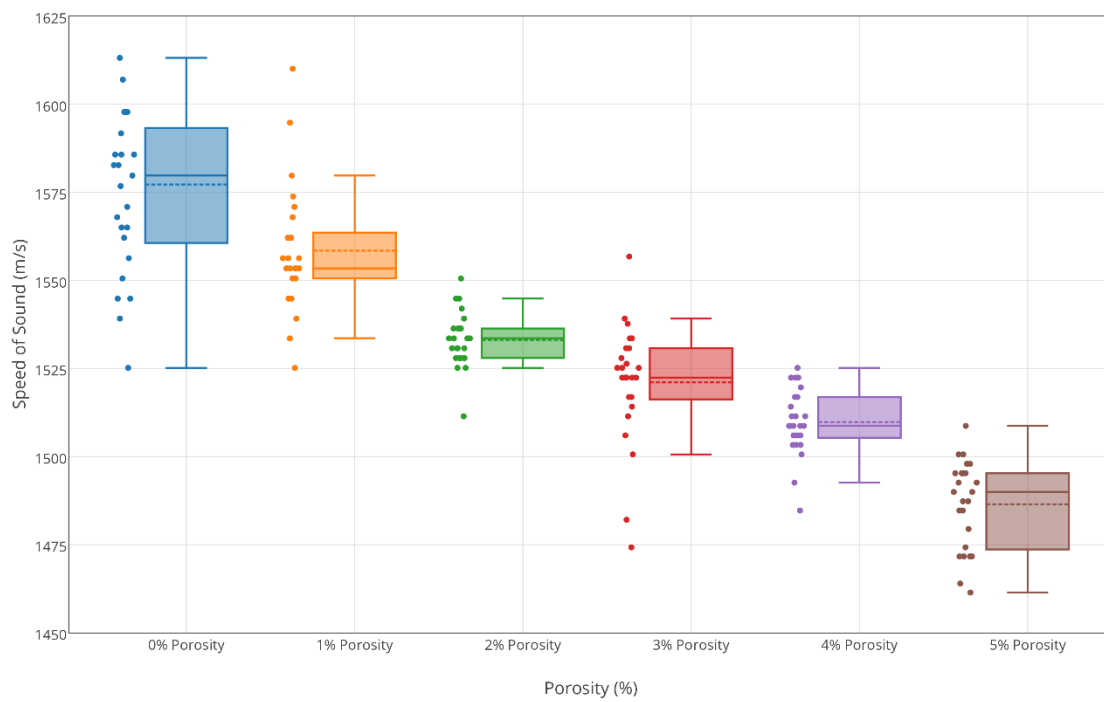
4.2.2.2 300mm

Speed of Transversal Sound Transmission Through 300mm of Pine Wood



4.2.2.3 400mm

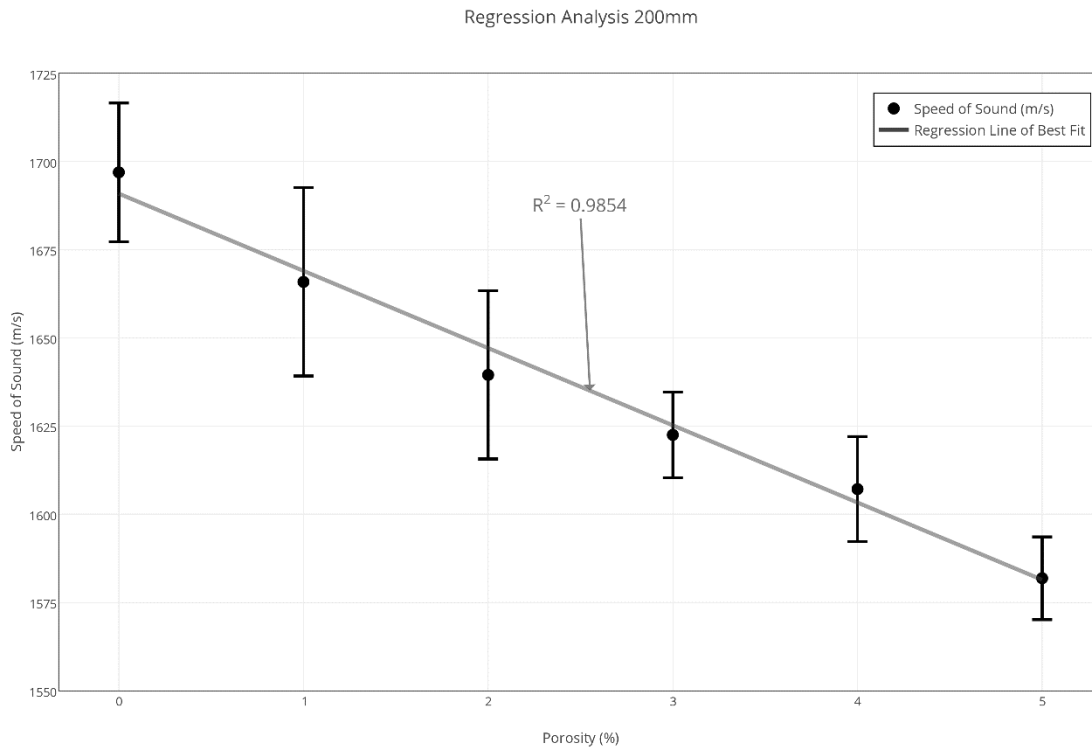
Speed of Transversal Sound Transmission Through 400mm of Pine Wood



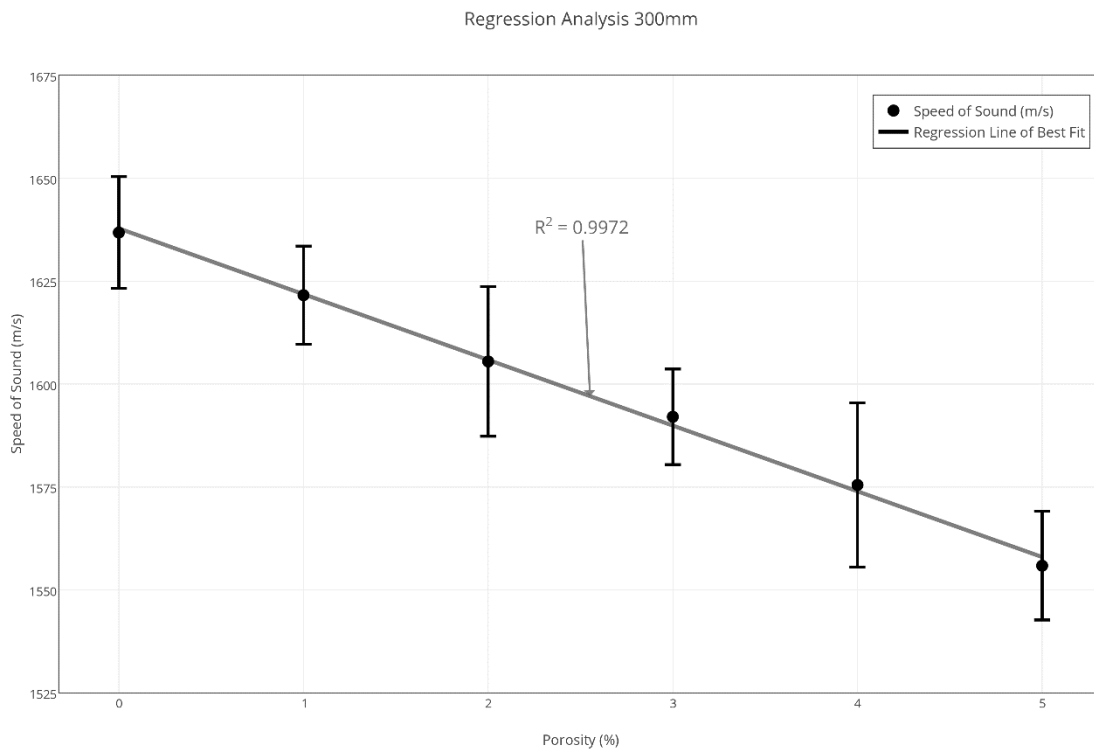
4.2.3 Regression Analysis

Regression analysis is shown for each distance tested across the 6 levels of porosity, to determine whether the speed of sound transmission follows a linear inverse correlation with porosity. The result takes into consideration the error bars of standard deviation.

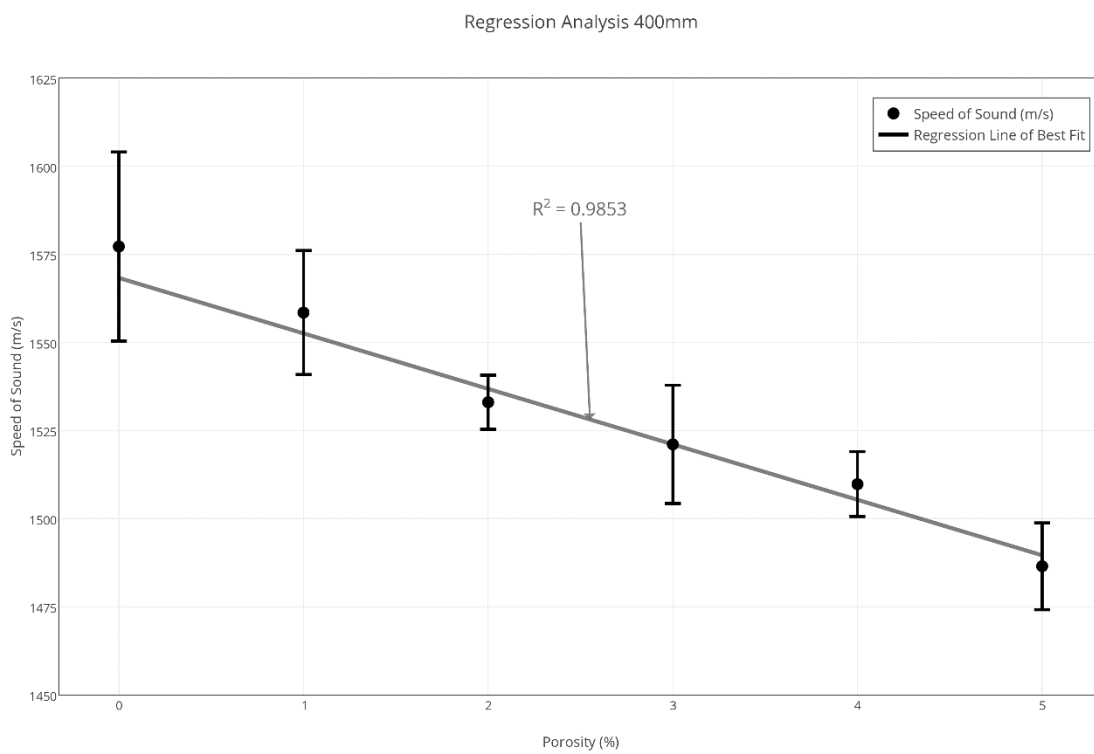
4.2.3.1 200mm



4.2.3.2 300mm



4.2.3.3 400mm



5 DISCUSSION OF RESULTS

This section contains analysis of the measurement results in reference to the research question for both preliminary measurements using a shaker as an excitation force, and measurements using an impact hammer as an excitation force.

5.1 Preliminary Measurements

In terms of signal transmission, results are similar to those found at much higher frequencies (100kHz) in bone replicas by Aygun *et al*(p. 7, 2014) whereby a negative amplitude peak or “fast wave” arrives before a positive “slow wave” which is seen in the results above. The fast wave arrives within the first 5ms (at all frequencies tested), while the slow wave is received directly afterwards. Subsequent waves are shown to be reflections of the input signal from each end of the dowel, being gradually attenuated at each cycle.

Results show that for all frequencies and distances tested there was no distinct change in signal attenuation between perforated and non-perforated wood, as the peaks for both perforated and solid dowel measurements are of the same amplitude, or the variation is too small to quantify. Although there is no noticeable attenuation, there is a clear indication of a change to the speed of sound transmission. The addition of perforations has caused the signal to travel slower through the wooden dowel, which can be seen by examining the perforated signal, shifting to the right of the non-perforated measurements in the plots above. Between 0ms and 20ms the signals are in phase with each other, showing that they have been received by the accelerometer simultaneously and that the shift is not caused by varying arrival time. By 40ms there is a noticeable shift in the perforated signal, delayed by around 5ms, indicating that the signal is travelling slower than through solid wood. This shift continues to increase with time, as it is closer to a 10ms difference at 80ms.

In order to quantify the time shift, measurements can be carried out to identify the arrival time of the input signal compared output signal, from which the transmission time (m/s) can be calculated using the distance between transducers (shown below). During this test the sampling rate of the oscilloscope was too low to reliably determine this time, but repeated measurements using a more powerful data acquisition system would provide more accurate results.

$$Speed (m/s) = \frac{Distance (m)}{Time (s)}$$

Higher frequency measurements (especially 100Hz) are more difficult to analyse due to increased variability, however they do still clearly show a speed shift in line with the more consistent low frequency results. Measurements carried out between 20cm and 40cm show a good signal level received by the accelerometer, while the 50cm result is beginning to diminish in comparison to the input signal level.

5.2 Impact Hammer Measurements

As shown in the preliminary measurements, a low amplitude “fast wave” is seen to arrive before the much higher amplitude signal in all of the measurements taken. This wave is used to calculate the speed of sound transmission as it is the first deviation from the noise floor of the acquisition system, and represents the impact from the hammer as a change in acceleration.

Results show that an increase in porosity causes a reduction to the speed of sound transmission, with an average change of -19.12 ± 5.68 m/s across three distances (200, 300, and 400mm) and 6 different porosity increments of 1%. Regression analysis shows that the change is very close to linear, with an average r^2 value of $r^2=0.98931$ across the 3 distances measured. Statistical analysis has shown that for the 1% incremental changes (e.g. 0% to 1%) the variances in the data sets are equal in 6, and unequal in 9. Subsequent t- tests assuming either equal or unequal variance depending on f-test results have shown that the null hypothesis can be rejected, as there is a high statistically significant difference between the means, with all results returning a p-value of <0.01 . The full statistical data set can be found in Appendix 8.2. The variation in the speed of sound transmission between each distance tested of 1696.95 ± 19.69 m/s at 200mm, 1636 ± 13.59 m/s at 300mm, and 1577.26 ± 26.81 m/s at 400mm, is likely due to the small differences in accelerometer placement and impact location, but could also be due to the variation in the wood, being an anisotropic structure with the possibility of different transmission paths in each section. The speed of sound in pine wood measured transversally using an ultrasonic method has been shown to be around 1600m/s (McDonald, 1978) which matches up well with the average SOS measured in this study of 1637.01 ± 48.87 m/s.

For calculating the speed of sound transmission the rest of the received signal and its reflections from the boundaries of the sample have been ignored, but reflections can be analysed further to reveal more potentially useful properties of the sample. Unfortunately the developed testing system is not capable of capturing this information due to the maximum number of samples that can be saved within a single block of data. If the current data was analysed using FFT the frequency resolution would not be high enough to detect the resonant frequency, or to determine whether it is affected by variations in porosity. The LabView system is capable of capturing this data if a more powerful acquisition hardware is used in the future, as well as carrying out the frequency analysis upon capture.

The introduction of an impact hammer (as opposed to a shaker in the preliminary measurement system) has introduced additional variation when striking the sample. The force applied to the surface of the sample and the location struck vary for each measurement, as well as the placement of the accelerometer after each increase in porosity, which causes uncertainty. For the measurements taken in this experiment the test was repeated 25 times at each location, in order to quantify the variation, but it may be possible to reduce the amount of variation by better controlling the input parameters. In order to control input force a spring mechanism may be developed, this would eliminate variations in SOS results from impacts of different force. There is also less chance of accidental damage to the sample from an overly forceful impact. A spring loaded impact hammer and accelerometer testing probe has been shown to be capable of detecting the wave speed in a wooden sample, the results of which can be compared to a known healthy sample to measure the extent of decay (Graham and Helsing, 1979). This is similar to the use of a phantom in ultrasonic osteoporosis testing, and could also be applied to a low frequency method in a similar way to Cheng (1995).

To control the distance between the transducers a digital caliper system may be used that measures the exact distance between transducers, and sends this data to the LabView system, so that the calculation is always using the correct separation distance. The difference in transmission time between 2 accelerometers could also be used, which would eliminate variations caused by the location of the impact hammer as suggested by Ross (2015).

Greater bit depth in the acquisition system (currently 8 bit) would allow for more reliable acquisition at low input level (less force from the impact hammer) which would be less damaging to a sample or person being tested. A lower sensitivity accelerometer may also help when analysing the signal in the frequency domain, as the majority of the signal is lost due to clipping when attempting to achieve a suitable signal level for the first received peak. The lower sensitivity may have a negative affect though, as the very first received signal is a much lower level than the majority of signal, and may be lost in the noise floor of the system.

6 CONCLUSIONS

When reflecting on the initial research question, it has been possible to measure the speed of sound transmission through a sample using a non-destructive measurement method, and it has also been possible to measure the change in this speed due to an increase in porosity. From these results it is possible to reject the null hypothesis and accept the alternative; that this test system is capable of reliably distinguishing between porosity changes in a wooden dowel.

Further research may be able to increase the accuracy of the system, to be used to measure even smaller variations in porosity using the speed of sound transmission. The system could then be applied to measure the properties of wood in-situ, for example to analyse the extent of wood worm damage without damaging the sample. Unfortunately it has not been possible to analyse any frequency based variations caused by porosity, due to the limitations of the acquisition hardware, but the design of the system allows for this in future development.

The system has an advantage over other testing systems, as it does not suffer from high signal attenuation in comparison to ultrasonic methods, and it does not require the sample to be immersed in a fluid as with the most common porosity measurement. With a low impact force from a hammer this can be considered a non-destructive method that can be used in-situ for investigating the structural properties of wood.

As Aygun *et al.* (2014) suggested, a system such as this could be developed for detecting the early signs of osteoporosis, although there are a number of issues that would need to be addressed. Firstly, the systems accuracy and reliability would need to be improved by modifying the acquisition hardware, and the method of transducer attachment. The system would then need to be tested on human participants to evaluate the extent to which the results found during this study are relevant, whether the response of the bone and soft tissue can be measured in the same way as wood. Participants with varying levels of previously known osteoporosis would need to be tested in order to detect a difference in the speed of sound transmission, ranging from healthy to osteoporotic. The measurement is further complicated by the soft tissue and skin attenuation that would vary between test subjects, potentially making it more difficult to accurately determine the properties of the bone. A large database of results would need to be gathered for people of different ages, races, etc. as the speed of sound transmission is unlikely to be the same for everyone.

In comparison to other methods used for osteoporosis detection, this system is considerably less expensive than DXA and QCT methods and would not require a specialised operator, allowing it to be installed in doctors surgeries and health centres. This would therefore allow for early osteoporosis detection as part of regular check-ups, potentially allowing patients access to treatment earlier. This method may also be less expensive than ultrasound methods, and could be more easily placed in other locations than the calcaneus, such as the tibia, as shown by measurements carried out by M. S. Holi (2003).

7 REFERENCES

Aygun, Haydar. Barlow, Chris. (2015). *Ultrasonic wave propagation through porous materials at different angles of propagation*. Applied Acoustics, February 2015, 99, pp. 6-11.

Aygun, Haydar. Barlow, Chris. (2014). *Behaviour of ultrasonic waves in porous rigid materials: an anisotropic Biot-Attenborough model*. Journal of Physics: Conference Series 581 (2015) 012006.

Bekhhta, P. A. Niemz, P. Kucera, L. (2014). *The study of sound propagation in the wood-based composite materials*. 12th International Symposium on Nondestructive of Wood, At Sopron, 13-15 September 2000, pp.33-41.

Bell, E.R.; Peck, E.C.; Krueger, N.T. 1954. Modulus of elasticity of wood determined by dynamic methods. Rep. 1977. Madison, WI: U.S. Department of Agriculture, Forest Service, Forest Products Laboratory.

Bertholf, L.D. 1965. Use of elementary stress wave theory for prediction of dynamic strain in wood. Bull. 291. Pullman, WA: Washington State University, College of Engineering.

Blake, G.M. and Fogelman, I. (1997) 'Technical principles of dual energy x-ray absorptiometry', *Seminars in Nuclear Medicine*, 27(3), pp. 210–228.

British Orthopaedic Association (2007) *The Care of Patients with Fragility Fracture ('Blue Book')*. .

Burge, R.T., Worley, D., Johansen, A., Bhattacharyya, S. and Bose, U. (2001) *The cost of osteoporotic fractures in the UK: Projections for 2000–2020*. (4 Vols). Informa Healthcare.

British Standards Institution. (1993). 623-2. Advanced technical ceramics. Monolithic ceramics. General and textural properties. Determination of density and porosity. London: British Standards Institution.

Cheng, S., Timonen, J. and Suominen, H. (1995) 'Elastic wave propagation in bone: Methodology', *Journal of Biomechanics*, 28(4), pp. 471–478.

Christiansen, C. (1995) 'Osteoporosis: Diagnosis and management today and tomorrow', *Bone.*, 17(5).

Chuang, S.-T. and Wang, S.-Y. (2001) 'Evaluation of standing tree quality of Japanese cedar grown with different spacing using stress-wave and ultrasonic-wave methods', *Journal of Wood Science*, 47(4), pp. 245–253.

Cooper, C. and Christodoulou, C. (2003) 'What is osteoporosis?', *Postgraduate Medical Journal*, 79(929), pp. 133–138.

Dupont, Thomas. Leclair, Philippe. Panneton, Raymond. (2013) Acoustic methods for measuring the porosities of porous materials incorporating dead-end pores. J. Acoust. Soc. Am. 133, 2136 (2013). Acoustical Society of America.

Engelke, K., Adams, J.E., Armbrrecht, G., Augat, P., Bogado, C.E., Bouxsein, M.L., Felsenberg, D., Ito, M., Prevrhal, S., Hans, D.B. and Lewiecki, M.E. (2007) 'Position statement clinical use of quantitative computed tomography and peripheral quantitative computed tomography in the management of osteoporosis in adults: The 2007 ISCD official positions', *Journal of Clinical Densitometry: Assessment of Skeletal Health*, 11(1), pp. 123–162.

Ethnicity and national identity in England and wales 2011 (2015) Available at: http://www.ons.gov.uk/ons/dcp171776_290558.pdf (Accessed: 5 December 2015).

Faulkner, K.G., McClung, M.R., Coleman, L.J., Kingston-Sandah, E. and Kingston-Sandah, E. (1994) 'Quantitative ultrasound of the heel: Correlation with densitometric measurements at different skeletal sites', *Osteoporosis International*, 4(1), pp. 42–47.

Fellah, Z. E. A. *et al.* (2003) *Measuring the porosity and the tortuosity of porous materials via reflected waves at oblique incidence*. J. Acoust. Soc. Am. 113 (5), May 2003. Acoustical Society of America.

Fellah, Z. E. A. Fellah, M. Depollier, C. (2013). *Transient Acoustic Wave Propagation in Porous Media*. Modeling and Measurement Methods for Acoustic Microdevices. Chapter 6. ISBN 978-953-51-1189-4, Published: August 28, 2013.

Fewtrell, M.S. (2003) 'Bone densitometry in children assessed by dual x ray absorptiometry: Uses and pitfalls', *Archives of Disease in Childhood*, 88(9), pp. 795–798.

Frost, M.L., Blake, G.M. and Fogelman, I. (2001) 'Quantitative ultrasound and bone mineral density are equally strongly associated with risk factors for osteoporosis', *Journal of Bone and Mineral Research*, 16(2), pp. 406–416.

Glüer, C.-C. (1997) 'Quantitative ultrasound techniques for the assessment of osteoporosis: Expert agreement on current status', *Journal of Bone and Mineral Research*, 12(8).

Graham, R. D. G. G. Helsing. (1979) *Wood pole maintenance manual: Inspection and supplemental treatment of Douglas-fir and western redcedar poles*, Res. Bull. 24. Res. Lab., Oregon State University, Corvallis, Oregon.

International Organization for Standardization. (1999). 2738. Sintered metal materials, excluding hardmetals -- Permeable sintered metal materials -- Determination of density, oil content and open porosity. International Organization for Standardization.

Kanis, J.A., Melton, J.L., Christiansen, C.L., Khaltsev, N. and Johnston, C.C. (2009) 'Perspective: The diagnosis of osteoporosis', *Journal of Bone and Mineral Research*, 9(8).

Kaiserlik, J.H.; Pellerin, R.F. 1977. Stress wave attenuation as an indicator of lumber strength. *Forest Products Journal*. 27(6): 39–43.

Langton, C.M. (2011) 'The 25th anniversary of BUA for the assessment of osteoporosis: Time for a new paradigm?', *Proceedings of the Institution of Mechanical Engineers Part H Journal of Engineering in Medicine*, 225(2), pp. 113–25.

Laskey, M.A. (1996) 'Dual-energy x-ray absorptiometry and body composition', *Nutrition*, 12(1), pp. 45–51.

McDonald KA (1978) Lumber defect detection by ultrasonics. Res Pap 311. Forest Products Laboratory, USDA, Washington, DC.

Michaels, Jennifer E. Michaels, Thomas E. Jonsson, Staffen. (1993). Ultrasonic Methods for Detection of Micro Porosity in Composite Materials. Review of progress in quantitative non-destructive evaluation, Vol. 12. New York: Plenum Press 1993.

Moavenzadeh, F. (1990) *Concise encyclopedia of building and construction materials*. MIT Press.

Pellerin, R.F.; De Groot, R.C.; Esenther, G.R. 1985. Nondestructive stress wave measurements of decay and termite attack in experimental wood units. In: Proceedings, 5th nondestructive testing of wood symposium; 1985 September 9–11; Pullman, WA. Pullman, WA: Washington State University: 319–353

Prins, S.H. (1997) 'The role of quantitative ultrasound in the assessment of bone: a review', *Clinical Physiology Jan 1998*, 18(1), pp. 3–15.

Rho, J.-Y., Kuhn-Spearing, L. and Zioupos, P. (1998) 'Mechanical properties and the hierarchical structure of bone', *Medical Engineering & Physics*, 20(2), pp. 92–102.

Ross, R.J. 1985. Stress wave propagation in wood products. In: Proceedings, 5th nondestructive testing of wood symposium; 1985 September 9–11; Pullman, WA. Pullman, WA: Washington State University: 291–318.

Ross, R.J. and USDA Forest Service (2015) *Nondestructive evaluation of wood*. Available at: http://www.fpl.fs.fed.us/documnts/fplgtr/fpl_gtr238.pdf (Accessed: 9 February 2016).

Rutherford, P.S.; Hoyle, R.J.; De Groot, R.C.; Pellerin, R.F. 1987. Dynamic vs. static MOE in the transverse direction in wood. In: Proceedings, 6th nondestructive testing of wood symposium; 1987 September 14–16; Pullman, WA. Pullman, WA: Washington State University: 67–80.

Singer, A. (2006) 'Osteoporosis diagnosis and screening', *Clinical Cornerstone*, 8(1).

S, H., G.T, H. and R, C. (1974) 'Acoustic emission and diagnosis of osteoporosis', 1974 Ultrasonics Symposium: IEEE. Available at: http://ieeexplore.ieee.org/xpls/abs_all.jsp?arnumber=1533230&tag=1 (Accessed: 15 February 2016).

S, H.M. and S, R. (2003) 'In vivo assessment of osteoporosis in women by impulse response technique', TENCON 2003. Conference on Convergent Technologies for the Asia-Pacific Region: IEEE. Available at: http://ieeexplore.ieee.org/xpls/abs_all.jsp?arnumber=1273147&tag=1 (Accessed: 15 February 2016).

S, H. and R.G, C. (1975) 'Acoustic emission techniques in the development of a Diagnostic tool for osteoporosis', IEEE. Available at: http://ieeexplore.ieee.org/xpls/abs_all.jsp?arnumber=1533401&tag=1 (Accessed: 15 February 2016).

Unosson, Johanna E. Persson, Cecilia. Engqvist, Haken. (2014). An evaluation of methods to determine the porosity of calcium phosphate cements. *Journal of Biomedical Materials Research. Part B - Applied biomaterials*, ISSN 1552-4973, E-ISSN 1552-4981, Vol. 103, no 1, 62-71.

Yim-Bun P. Kwan. J. R. Alcock. (2002) The impact of water impregnation methods on the accuracy of open porosity measurements. *Journal of Materials Science* 37, 2557-2561. Cranfield University, UK.

8 APPENDICIES

8.1 Matlab code for plotting preliminary measurement results

```

clear all
close all
format long

load test40hz1.txt
load test40hz2.txt
load test40hz3.txt

load test40hz1h.txt
load test40hz2h.txt
load test40hz3h.txt

% Read in input/output values from file

time      = test40hz1(:,1);

input1    = test40hz1(:,2);
input2    = test40hz2(:,2);
input3    = test40hz3(:,2);

output1   = test40hz1(:,3);
output2   = test40hz2(:,3);
output3   = test40hz3(:,3);

output1h  = test40hz1h(:,3);
output2h  = test40hz2h(:,3);
output3h  = test40hz3h(:,3);

% Average the 3 measurements for input/output

inputaverage = (input1+input2+input3)/3;
outputaverage = (output1+output2+output3)/3;
outputaverageh = (output1h+output2h+output3h)/3;

% Plots

plot(time,inputaverage,'b-.','LineWidth',2); hold on;
plot(time,outputaverage,'r','LineWidth',2); hold on;
plot(time,outputaverageh,'black--','LineWidth',2); hold on;
axis([-20 100 -500 500]);

xlabel('Time, (ms)')
ylabel('Amplitude, (mV)')
legend('Input','Output Without Perforation','Output With Perforation');
set(findall(gcf,'-property','fontSize'),'fontSize',10)
set(legend,'FontSize',8);
grid on
set(gca,'dataaspectratio',[1 12 1])
export_fig 20cm40hz -png -transparent -r600 -painters -p0.02 -a1

```

8.2 Impact Measurement Results

8.2.1 Results at 200mm

0%		1%		2%		3%		4%		5%		
SOS (m/s)	Input (N)	SOS (m/s)	Input (N)	SOS (m/s)	Input (N)	SOS (m/s)	Input (N)	SOS (m/s)	Input (N)	SOS (m/s)	Input (N)	
1671.04	55.56	1632.03	63.56	1619.42	79.56	1657.83	63.56	1576.81	47.56	1565.04	51.56	
1671.04	67.56	1632.03	75.56	1600.88	67.56	1607.01	55.56	1588.75	47.56	1565.04	51.56	
1671.04	71.56	1632.03	67.56	1625.70	67.56	1607.01	51.56	1588.75	43.56	1565.04	55.56	
1671.04	59.56	1638.40	71.56	1698.10	67.56	1607.01	51.56	1588.75	51.56	1570.90	47.56	
1677.72	55.56	1638.40	75.56	1651.30	83.56	1607.01	59.56	1594.79	55.56	1570.90	51.56	
1684.46	71.56	1657.83	67.56	1600.88	67.56	1607.01	71.56	1600.88	51.56	1570.90	51.56	
1684.46	63.56	1657.83	71.56	1607.01	79.56	1613.19	59.56	1600.88	51.56	1576.81	55.56	
1684.46	55.56	1657.83	67.56	1644.83	75.56	1613.19	51.56	1607.01	63.56	1576.81	55.56	
1684.46	59.56	1657.83	79.56	1632.03	75.56	1613.19	55.56	1607.01	51.56	1576.81	51.56	
1684.46	91.56	1657.83	79.56	1644.83	79.56	1619.42	59.56	1607.01	43.56	1576.81	51.56	
1684.46	67.56	1657.83	71.56	1632.03	87.56	1619.42	63.56	1613.19	67.56	1576.81	51.56	
1691.25	67.56	1657.83	67.56	1657.83	95.56	1619.42	51.56	1613.19	51.56	1576.81	59.56	
1691.25	51.56	1657.83	67.56	1632.03	83.56	1619.42	51.56	1613.19	51.56	1576.81	51.56	
1691.25	67.56	1664.41	79.56	1644.83	75.56	1619.42	67.56	1613.19	51.56	1582.76	71.56	
1698.10	47.56	1664.41	63.56	1657.83	75.56	1625.70	59.56	1613.19	51.56	1582.76	55.56	
1705.00	79.56	1664.41	71.56	1671.04	71.56	1625.70	59.56	1619.42	67.56	1582.76	47.56	
1705.00	71.56	1664.41	67.56	1625.70	67.56	1625.70	67.56	1619.42	47.56	1582.76	59.56	
1711.96	51.56	1664.41	67.56	1657.83	79.56	1625.70	51.56	1625.70	55.56	1582.76	63.56	
1711.96	75.56	1671.04	83.56	1607.01	67.56	1625.70	71.56	1607.01	55.56	1594.79	47.56	
1711.96	71.56	1671.04	87.56	1619.42	71.56	1632.03	67.56	1625.70	51.56	1594.79	51.56	
1718.98	67.56	1684.46	79.56	1684.46	79.56	1632.03	67.56	1632.03	47.56	1594.79	47.56	
1726.05	63.56	1684.46	51.56	1644.83	67.56	1632.03	67.56	1613.19	55.56	1594.79	51.56	
1726.05	71.56	1705.00	75.56	1638.40	71.56	1632.03	71.56	1600.88	51.56	1600.88	67.56	
1733.18	83.56	1733.18	71.56	1644.83	79.56	1638.40	75.56	1632.03	51.56	1600.88	51.56	
1733.18	67.56	1740.38	71.56	1644.83	83.56	1638.40	79.56	1576.81	67.56	1607.01	59.56	
Average	1696.95	66.28	1665.88	71.88	1639.51	76.04	1622.52	62.12	1607.15	53.32	1581.89	54.44
SD (±)	19.70	10.16	26.71	7.33	23.85	7.27	12.12	8.23	14.93	6.60	11.69	6.04

8.2.2 F and T test Results 200mm

8.2.2.1 0% - 1%

F-Test Two-Sample for Variances		
	Variable 1	Variable 2
Mean	1665.88324	1696.952
Variance	742.9834218	404.1987
Observations	25	25
df	24	24
F	1.838163981	
P(F<=f) one-tail	0.071504484	
F Critical one-tail	1.983759568	

t-Test: Two-Sample Assuming Equal Variances		
	Variable 1	Variable 2
Mean	1696.95244	1665.883
Variance	404.1986621	742.9834
Observations	25	25
Pooled Variance	573.5910419	
Hypothesized Mean Difference	0	
df	48	
t Stat	4.586526395	
P(T<=t) one-tail	1.62185E-05	
t Critical one-tail	1.677224196	
P(T<=t) two-tail	3.2437E-05	
t Critical two-tail	2.010634758	

8.2.2.2 1% - 2%

F-Test Two-Sample for Variances		
	Variable 1	Variable 2
Mean	1665.88324	1639.51324
Variance	742.9834218	592.3697682
Observations	25	25
df	24	24
F	1.254256145	
P(F<=f) one-tail	0.291644791	
F Critical one-tail	1.983759568	

t-Test: Two-Sample Assuming Equal Variances		
	Variable 1	Variable 2
Mean	1665.88324	1639.51324
Variance	742.9834218	592.3697682
Observations	25	25
Pooled Variance	667.676595	
Hypothesized Mean Difference	0	
df	48	
t Stat	3.608129031	
P(T<=t) one-tail	0.000366832	
t Critical one-tail	1.677224196	
P(T<=t) two-tail	0.000733664	
t Critical two-tail	2.010634758	

8.2.2.3 2% - 3%

F-Test Two-Sample for Variances		
	Variable 1	Variable 2
Mean	1639.51324	1622.5192
Variance	592.3697682	153.0900019
Observations	25	25
df	24	24
F	3.869421652	
P(F<=f) one-tail	0.000768481	
F Critical one-tail	1.983759568	

t-Test: Two-Sample Assuming Unequal Variances		
	Variable 1	Variable 2
Mean	1639.51324	1622.5192
Variance	592.3697682	153.0900019
Observations	25	25
Hypothesized Mean Difference	0	
df	36	
t Stat	3.112107104	
P(T<=t) one-tail	0.001813934	
t Critical one-tail	1.688297714	
P(T<=t) two-tail	0.003627869	
t Critical two-tail	2.028094001	

8.2.2.4 3% - 4%

F-Test Two-Sample for Variances		
	Variable 1	Variable 2
Mean	1607.1522	1622.5
Variance	232.2413734	153.09
Observations	25	25
df	24	24
F	1.517025087	
P(F<=f) one-tail	0.157046514	
F Critical one-tail	1.983759568	

t-Test: Two-Sample Assuming Equal Variances		
	Variable 1	Variable 2
Mean	1622.5192	1607.2
Variance	153.0900019	232.24
Observations	25	25
Pooled Variance	192.6656877	
Hypothesized Mean Difference	0	
df	48	
t Stat	3.914190056	
P(T<=t) one-tail	0.000142835	
t Critical one-tail	1.677224196	
P(T<=t) two-tail	0.000285669	
t Critical two-tail	2.010634758	

8.2.2.5 4% - 5%

F-Test Two-Sample for Variances		
	<i>Variable 1</i>	<i>Variable 2</i>
Mean	1607.1522	1581.9
Variance	232.2413734	142.38
Observations	25	25
df	24	24
F	1.63116451	
P(F<=f) one-tail	0.118934645	
F Critical one-tail	1.983759568	

t-Test: Two-Sample Assuming Equal Variances		
	<i>Variable 1</i>	<i>Variable 2</i>
Mean	1607.1522	1581.9
Variance	232.2413734	142.38
Observations	25	25
Pooled Variance	187.3095128	
Hypothesized Mean Difference	0	
df	48	
t Stat	6.526731804	
P(T<=t) one-tail	1.95659E-08	
t Critical one-tail	1.677224196	
P(T<=t) two-tail	3.91318E-08	
t Critical two-tail	2.010634758	

8.2.3 Results at 300mm

	0%		1%		2%		3%		4%		5%	
	SOS (m/s)	Input (N)										
	1613.19	59.56	1604.96	55.56	1572.86	55.56	1565.04	59.56	1557.29	51.56	1534.50	47.56
	1617.34	51.56	1621.51	59.56	1565.04	63.56	1572.86	51.56	1568.94	55.56	1538.25	71.56
	1617.34	51.56	1613.19	51.56	1604.96	67.56	1572.86	59.56	1553.45	47.56	1542.02	63.56
	1625.70	51.56	1634.14	71.56	1613.19	79.56	1576.81	47.56	1565.04	51.56	1542.02	63.56
	1625.70	51.56	1613.19	51.56	1604.96	75.56	1584.75	51.56	1565.04	47.56	1542.02	67.56
	1625.70	51.56	1613.19	59.56	1609.07	71.56	1588.75	63.56	1572.86	67.56	1542.02	63.56
	1625.70	51.56	1609.07	51.56	1576.81	55.56	1588.75	47.56	1600.88	75.56	1545.81	71.56
	1625.70	55.56	1617.34	59.56	1600.88	67.56	1588.75	51.56	1634.14	55.56	1545.81	55.56
	1629.91	55.56	1634.14	59.56	1613.19	67.56	1588.75	63.56	1576.81	59.56	1545.81	67.56
	1629.91	67.56	1629.91	55.56	1609.07	79.56	1588.75	51.56	1596.82	67.56	1545.81	63.56
	1629.91	71.56	1604.96	51.56	1617.34	83.56	1588.75	51.56	1580.77	55.56	1545.81	67.56
	1634.14	63.56	1617.34	59.56	1625.70	91.56	1592.77	51.56	1561.16	51.56	1549.62	79.56
	1634.14	55.56	1604.96	51.56	1617.34	75.56	1592.77	63.56	1576.81	63.56	1557.29	79.56
	1634.14	71.56	1646.98	87.56	1609.07	59.56	1596.82	67.56	1600.88	67.56	1561.16	67.56
	1638.40	59.56	1638.40	63.56	1600.88	91.56	1596.82	67.56	1553.45	51.56	1561.16	63.56
	1642.68	75.56	1621.51	47.56	1600.88	79.56	1596.82	75.56	1596.82	71.56	1565.04	87.56
	1642.68	63.56	1642.68	75.56	1596.82	83.56	1596.82	71.56	1576.81	47.56	1565.04	79.56
	1642.68	63.56	1625.70	67.56	1609.07	79.56	1596.82	47.56	1557.29	47.56	1565.04	75.56
	1646.98	63.56	1609.07	47.56	1655.65	59.56	1596.82	71.56	1549.62	55.56	1565.04	67.56
	1655.65	63.56	1634.14	63.56	1596.82	79.56	1596.82	63.56	1580.77	63.56	1565.04	79.56
	1655.65	67.56	1621.51	67.56	1625.70	79.56	1600.88	63.56	1604.96	79.56	1568.94	67.56
	1655.65	63.56	1621.51	51.56	1609.07	63.56	1600.88	47.56	1568.94	51.56	1572.86	83.56
	1655.65	75.56	1609.07	63.56	1592.77	75.56	1600.88	51.56	1561.16	55.56	1572.86	63.56
	1655.65	67.56	1629.91	63.56	1621.51	59.56	1609.07	87.56	1557.29	51.56	1576.81	67.56
	1660.02	59.56	1621.51	63.56	1588.75	59.56	1621.51	75.56	1568.94	63.56	1580.77	63.56
Average	1636.81	61.32	1621.60	60.04	1605.50	72.20	1592.05	60.20	1575.48	58.28	1555.86	69.16
SD (\pm)	13.59	7.60	11.91	9.14	18.15	10.53	11.61	10.59	19.97	9.03	13.21	8.76

8.2.4 F and T-test Results 300mm

8.2.4.1 0% - 1%

F-Test Two-Sample for Variances		
	Variable 1	Variable 2
Mean	1636.80772	1621.596
Variance	192.451884	147.808
Observations	25	25
df	24	24
F	1.30203965	
P(F<=f) one-tail	0.2614485	
F Critical one-tail	1.98375957	

t-Test: Two-Sample Assuming Equal Variances		
	Variable 1	Variable 2
Mean	1636.80772	1621.596
Variance	192.451884	147.808
Observations	25	25
Pooled Variance	170.129945	
Hypothesized Mean Difference	0	
df	48	
t Stat	4.12316188	
P(T<=t) one-tail	7.3654E-05	
t Critical one-tail	1.6772242	
P(T<=t) two-tail	0.00014731	
t Critical two-tail	2.01063476	

8.2.4.2 1% - 2%

F-Test Two-Sample for Variances		
	Variable 1	Variable 2
Mean	1605.496	1621.596
Variance	343.0346	147.808
Observations	25	25
df	24	24
F	2.320812	
P(F<=f) one-tail	0.022099	
F Critical one-tail	1.98376	

t-Test: Two-Sample Assuming Unequal Variances		
	Variable 1	Variable 2
Mean	1621.596	1605.496
Variance	147.808	343.0346
Observations	25	25
Hypothesized Mean Difference	0	
df	41	
t Stat	3.633659	
P(T<=t) one-tail	0.000385	
t Critical one-tail	1.682878	
P(T<=t) two-tail	0.000771	
t Critical two-tail	2.019541	

8.2.4.3 2% - 3%

F-Test Two-Sample for Variances		
	Variable 1	Variable 2
Mean	1605.496	1592.05
Variance	343.0346	140.337
Observations	25	25
df	24	24
F	2.444369	
P(F<=f) one-tail	0.016484	
F Critical one-tail	1.98376	

t-Test: Two-Sample Assuming Unequal Variances		
	Variable 1	Variable 2
Mean	1605.496	1592.05
Variance	343.0346	140.337
Observations	25	25
Hypothesized Mean Difference	0	
df	41	
t Stat	3.057296	
P(T<=t) one-tail	0.001961	
t Critical one-tail	1.682878	
P(T<=t) two-tail	0.003922	
t Critical two-tail	2.019541	

8.2.4.4 3% - 4%

F-Test Two-Sample for Variances		
	Variable 1	Variable 2
Mean	1575.47656	1592.052
Variance	415.3480781	140.3367
Observations	25	25
df	24	24
F	2.959654804	
P(F<=f) one-tail	0.005078869	
F Critical one-tail	1.983759568	

t-Test: Two-Sample Assuming Unequal Variances		
	Variable 1	Variable 2
Mean	1592.05236	1575.477
Variance	140.3366627	415.3481
Observations	25	25
Hypothesized Mean Difference	0	
df	39	
t Stat	3.515849422	
P(T<=t) one-tail	0.000564241	
t Critical one-tail	1.684875122	
P(T<=t) two-tail	0.001128482	
t Critical two-tail	2.02269092	

8.2.4.5 4% - 5%

F-Test Two-Sample for Variances		
	<i>Variable 1</i>	<i>Variable 2</i>
Mean	1575.477	1555.863
Variance	415.3481	181.8187
Observations	25	25
df	24	24
F	2.284408	
P(F<=f) one-tail	0.024109	
F Critical one-tail	1.98376	

t-Test: Two-Sample Assuming Unequal Variances		
	<i>Variable 1</i>	<i>Variable 2</i>
Mean	1575.477	1555.863
Variance	415.3481	181.8187
Observations	25	25
Hypothesized Mean Difference	0	
df	42	
t Stat	4.013128	
P(T<=t) one-tail	0.000121	
t Critical one-tail	1.681952	
P(T<=t) two-tail	0.000242	
t Critical two-tail	2.018082	

8.2.5 Results at 400mm

	0%		1%		2%		3%		4%		5%	
	SOS (m/s)	Input (N)	SOS (m/s)	Input (N)	SOS (m/s)	Input (N)	SOS (m/s)	Input (N)	SOS (m/s)	Input (N)	SOS (m/s)	Input (N)
	1525.20	175.56	1525.20	115.56	1525.20	111.56	1533.57	111.56	1484.71	75.56	1461.43	67.56
	1539.19	159.56	1533.57	111.56	1550.57	111.56	1525.20	95.56	1492.64	67.56	1463.98	59.56
	1544.86	127.56	1539.19	79.56	1533.57	111.56	1533.57	83.56	1500.65	67.56	1471.69	63.56
	1544.86	183.56	1544.86	91.56	1536.38	95.56	1522.43	79.56	1503.34	75.56	1471.69	59.56
	1550.57	159.56	1544.86	111.56	1527.98	99.56	1525.20	95.56	1503.34	71.56	1471.69	63.56
	1556.33	143.56	1550.57	111.56	1544.86	115.56	1516.93	83.56	1503.34	67.56	1471.69	55.56
	1562.12	191.56	1550.57	91.56	1544.86	119.56	1514.19	95.56	1506.03	67.56	1474.27	67.56
	1565.04	135.56	1553.45	111.56	1536.38	119.56	1506.03	71.56	1506.03	75.56	1479.47	67.56
	1565.04	147.56	1553.45	67.56	1525.20	87.56	1530.77	83.56	1506.03	67.56	1484.71	79.56
	1567.96	127.56	1553.45	107.56	1533.57	83.56	1522.43	75.56	1508.74	67.56	1484.71	67.56
	1570.90	191.56	1553.45	111.56	1536.38	99.56	1522.43	79.56	1508.74	75.56	1487.34	71.56
	1576.81	163.56	1553.45	119.56	1527.98	95.56	1556.81	115.56	1508.74	59.56	1487.34	79.56
	1579.78	167.56	1553.45	99.56	1542.02	111.56	1537.71	107.56	1508.74	63.56	1489.98	67.56
	1582.76	131.56	1556.33	123.56	1539.19	107.56	1482.09	79.56	1508.74	63.56	1489.98	75.56
	1582.76	211.56	1556.33	115.56	1533.57	99.56	1530.77	83.56	1511.46	95.56	1492.64	71.56
	1585.75	147.56	1556.33	115.56	1536.38	99.56	1522.43	79.56	1511.46	95.56	1492.64	75.56
	1585.75	135.56	1562.12	99.56	1530.77	87.56	1511.46	83.56	1511.46	79.56	1495.30	83.56
	1585.75	179.56	1562.12	95.56	1530.77	95.56	1474.27	71.56	1514.19	71.56	1495.30	79.56
	1591.77	151.56	1562.12	103.56	1527.98	99.56	1539.19	87.56	1516.93	95.56	1495.30	75.56
	1597.83	151.56	1567.96	99.56	1533.57	99.56	1500.65	83.56	1516.93	67.56	1495.30	79.56
	1597.83	95.56	1570.90	119.56	1527.98	99.56	1526.38	87.56	1519.68	79.56	1497.97	79.56
	1597.83	143.56	1573.85	115.56	1530.77	91.56	1527.98	83.56	1522.43	87.56	1497.97	71.56
	1607.01	143.56	1579.78	107.56	1530.77	95.56	1522.43	87.56	1522.43	91.56	1500.65	87.56
	1613.19	151.56	1594.79	127.56	1527.98	95.56	1525.20	87.56	1522.43	75.56	1500.65	91.56
	1654.56	131.56	1610.10	131.56	1511.46	91.56	1516.93	79.56	1525.20	83.56	1508.74	87.56
Average	1577.26	153.96	1558.49	107.40	1533.04	101.00	1521.08	86.92	1509.78	75.56	1486.50	73.16
SD (±)	26.82	24.81	17.57	14.29	7.72	9.79	16.79	11.01	9.22	10.43	12.31	9.19

8.2.6 F and T-test results 400mm

8.2.6.1 0% - 1%

F-Test Two-Sample for Variances		
	Variable 1	Variable 2
Mean	1577.25792	1558.4898
Variance	749.0671376	321.6106293
Observations	25	25
df	24	24
F	2.329111881	
P(F<=f) one-tail	0.021665062	
F Critical one-tail	1.983759568	

t-Test: Two-Sample Assuming Unequal Variances		
	Variable 1	Variable 2
Mean	1577.25792	1558.4898
Variance	749.0671376	321.6106293
Observations	25	25
Hypothesized Mean Difference	0	
df	41	
t Stat	2.867882697	
P(T<=t) one-tail	0.003249706	
t Critical one-tail	1.682878002	
P(T<=t) two-tail	0.006499412	
t Critical two-tail	2.01954097	

8.2.6.2 1% - 2%

F-Test Two-Sample for Variances		
	Variable 1	Variable 2
Mean	1558.4898	1533.045
Variance	321.6106293	62.01691
Observations	25	25
df	24	24
F	5.185853739	
P(F<=f) one-tail	7.3593E-05	
F Critical one-tail	1.983759568	

t-Test: Two-Sample Assuming Unequal Variances		
	Variable 1	Variable 2
Mean	1558.4898	1533.045
Variance	321.6106293	62.01691
Observations	25	25
Hypothesized Mean Difference	0	
df	33	
t Stat	6.495605175	
P(T<=t) one-tail	1.1302E-07	
t Critical one-tail	1.692360309	
P(T<=t) two-tail	2.26039E-07	
t Critical two-tail	2.034515297	

8.2.6.3 2% - 3%

F-Test Two-Sample for Variances		
	Variable 1	Variable 2
Mean	1521.082	1533.045
Variance	293.6006	62.01691
Observations	25	25
df	24	24
F	4.734203	
P(F<=f) one-tail	0.000157	
F Critical one-tail	1.98376	

t-Test: Two-Sample Assuming Unequal Variances		
	Variable 1	Variable 2
Mean	1533.045	1521.082
Variance	62.01691	293.6006
Observations	25	25
Hypothesized Mean Difference	0	
df	34	
t Stat	3.171851	
P(T<=t) one-tail	0.001602	
t Critical one-tail	1.690924	
P(T<=t) two-tail	0.003205	
t Critical two-tail	2.032245	

8.2.6.4 3% - 4%

F-Test Two-Sample for Variances		
	Variable 1	Variable 2
Mean	1521.082	1509.776
Variance	293.6006	88.50592
Observations	25	25
df	24	24
F	3.317299	
P(F<=f) one-tail	0.002349	
F Critical one-tail	1.98376	

t-Test: Two-Sample Assuming Unequal Variances		
	Variable 1	Variable 2
Mean	1521.082	1509.776
Variance	293.6006	88.50592
Observations	25	25
Hypothesized Mean Difference	0	
df	37	
t Stat	2.891811	
P(T<=t) one-tail	0.003189	
t Critical one-tail	1.687094	
P(T<=t) two-tail	0.006379	
t Critical two-tail	2.026192	

8.2.6.5 4% - 5%

F-Test Two-Sample for Variances		
	<i>Variable 1</i>	<i>Variable 2</i>
Mean	1486.49544	1509.776
Variance	157.7942323	88.50592
Observations	25	25
df	24	24
F	1.782866429	
P(F<=f) one-tail	0.081931703	
F Critical one-tail	1.983759568	

t-Test: Two-Sample Assuming Equal Variances		
	<i>Variable 1</i>	<i>Variable 2</i>
Mean	1509.77628	1486.495
Variance	88.50591929	157.7942
Observations	25	25
Pooled Variance	123.1500758	
Hypothesized Mean Difference	0	
df	48	
t Stat	7.417137172	
P(T<=t) one-tail	8.45748E-10	
t Critical one-tail	1.677224196	
P(T<=t) two-tail	1.6915E-09	
t Critical two-tail	2.010634758	